TRANSIENT FLOW OF A SLURRY

A Thesis

Submitted to the Faculty of Graduate Studies

in Partial Fulfillment of the Requirements

for the Degree of

Master of Science

in the Department of

Chemistry and Chemical Engineering

University of Saskatchewan

by

Lanny Thomas Hubbard

Saskatoon, Saskatchewan

April, 1972

ABSTRACT

The effect of solid particles on pressure transients produced by flow changes was studied.

Water slurries of finely ground limestone were used at concentrations of 10%, 20%, 30%, and 35% by volume in experimental runs in a 2" pipeline. The experimental results were compared to computer simulations of the flow process.

The pressure transient associated with startup of a settled bed of solids was also studied. The results indicate a reduced sonic velocity and a unique underdamped oscillation for a system with a settled bed. No major difficulties were encountered in start-up of the settled bed in concentrations up to 35% by volume.

ACKNOWLEDGEMENTS

The author wishes to express his sincere thanks to Dr. C.A. Shook for his patient guidance and help throughout the course of this study and in the preparation of this thesis.

Thanks also, to the Saskatchewan Research Council - Engineering Division for their assistance and the use of some of their equipment in this research.

The financial contribution of the Canadian Transport Commission towards the purchase of equipment is gratefully acknowledged.

TABLE OF CONTENTS

LIST OF TABLES

LIST OF FIGURES

NOMENCLATURE

a	velocity of sound	ft/sec
A	acceleration	ft/sec^2
A_v	average	
c	volume fraction solids	
CV	valve coefficient	IGPM
CVO	initial valve coefficient	IGPM
C_m	Velocity of sound in mixture	ft/sec
D	pipe diameter	feet
E_L	modulus of elasticity of fluid	lb_f/ft^2
E_s	modulus of elasticity of solid	lb_f/ft^2
E_p	modulus of elasticity of pipe	lb_f/ft^2
f	friction factor (Fanning)	
F_c	corrected friction factor	
F_x	forces in x - direction	
g	acceleration of gravity	ft/sec^2
gc	conversion factor	$ft\text{-}lb_m/lb_f\text{-}sec^2$
L	length of pipeline	feet
lw_f	lost work due to friction	$(ft\text{-}lb_f)/lb_m$
M	mass	lb_m
N	number of calculation points in pipeline	
P	pressure	psig or psfg
ΔP	pressure change	psi
ρ	density	lb_m/ft^3
Q	volumetric flowrate	IGPM
Δt	time interval	seconds

t'	pipe thickness	feet
t	time	seconds
τ	ratio of CV/CVO	
τ_s	shear stress at the pipe wall	lb_f/ft^2
U_b	bulk flow velocity	ft/sec
v	velocity	ft/sec
W_s	shaft work	$(ft\text{-}lb_f)/lb_m$
X	position along pipeline	feet
Z	elevation above datum	feet

NOMENCLATURE OF COMPUTER PROGRAM

A	velocity of sound	ft/sec
CV	valve coefficient	IGPM
CVO	valve coefficient	IGPM
D	pipe diameter	feet
DELTX	segment of pipeline	feet
DELT	time interval	seconds
F	friction factor	
FC	corrected friction factor	
G	acceleration of gravity	ft/sec^2
GC	conversion factor	$(ft\text{-}lb_m)/lb_f\text{-}sec^2$
LT	Total pipeline length	feet
N	number of calculation points in pipeline	
P	pressure	psf
PP	pressure at a point, stored in memory	psi
PR	pressure at point R	psf
PS	pressure at point S	psf
PT	pressure at a point, stored in memory	psf
PTNOT	initial pressure at transducer	psi
PO	pressure drop across valve (initial)	psi
DELPO	Pressure drop across valve (initial or final steady state depending on starting conditions)	psi
T	time	seconds
TAU	ratio of CV/CVO	
TRANDS	distance of transducer from pipeline outlet	feet

V	velocity	ft/sec
VP	velocity stored in memory	ft/sec
VR	velocity at point R	ft/sec
VS	velocity at point S	ft/sec
VSS	Initial steady state velocity	ft/sec
XPC	particular pipeline segment (Chapter2.1.5)	feet
XCR	particular pipeline segment (Chapter2.1.5)	feet
ZO	elevation of head tank outlet above datum	feet
Z3	elevation of valve above datum	feet

CHAPTER 1. INTRODUCTION

The present work is a study of hydraulic transient behavior in solids pipeline systems. The pressure transient problem has been studied for pure Newtonian fluids, and mathematical equations describing simple systems with a high degree of accuracy have been available for some time. (References 1,3,4)

The increasing importance of slurry pipelines requires that a thorough understanding of transient flow in these systems be obtained. Until recently, very little investigation into the effect of solid particles on waterhammer has been made. The long term goal is to be able to predict the transient behavior of long slurry pipelines during flow changes and especially during start-up and shutdown.

It is possible that the behavior of systems involving homogeneous slurries could be predicted by the use of the waterhammer equations for water systems and the bulk properties of the slurry. The effect of stratification, and ultimately a stationary bed of solids in the system, must be determined.

To evaluate the difference in transient behavior between water and a typical slurry system, a 2" pipeline, 229 feet in length was constructed. Transient flow tests were planned with water and with limestone slurries of several different concentrations.

CHAPTER 2. THEORY

2.1 Equations governing the passage of a pressure wave.

The equations describing the propogation of a pressure wave in a single phase system are developed by Streeter and Lai. (Reference 1) The continuity equation and the equation of motion are transformed into total differential equations valid along "characteristic" lines. Using finite difference approximations a numerical solution can be made with a Digital Computer to give the fluid velocity and pressure at specified time intervals.

A rederivation of the continuity equation and the equation of motion will now be given to illustrate the physical principles of the experimental study. The derivation assumes negligible pipe elasticity, and applies strictly only to single phase systems. However corrections for the effect of pipe elasticity can be made, and the corrected equations will be applied to flowing slurries. Assuming the slurry behaves essentially as a homogeneous Newtonian fluid, the equations will give "predicted" or "theoretical" values of the pressure - time curves. These can be compared with the experimental values to assess the adequacy of the homogeneous Newtonian fluid assumption.

2.1.1 Continuity equation.

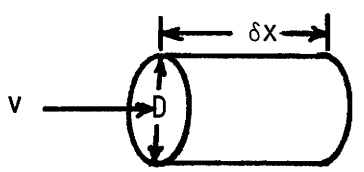

Figure 2.1 Schematic illustration of pipe segment

For the segment of the pipe shown in Figure 2.1

$$\text{Mass input} = \frac{\pi D^2}{4} v\rho \quad \text{.......... (2.1)}$$

$$\text{Mass output} = \frac{\pi D^2}{4} v\rho + \frac{\partial}{\partial x}\left(\frac{\pi D^2}{4} v\rho\right)\delta x \quad \text{.......... (2.2)}$$

$$\text{Accumulation} = \frac{\partial}{\partial t}\left(\frac{\pi D^2}{4}\rho\right)\delta x \quad \text{.......... (2.3)}$$

Therefore:

$$\frac{\partial}{\partial x}\left(\frac{\pi D^2}{4} v\rho\right) + \frac{\partial}{\partial t}\left(\frac{\pi D^2}{4}\rho\right) = 0 \quad \text{.......... (2.4)}$$

or

$$\rho\frac{\partial v}{\partial x} + v\frac{\partial \rho}{\partial x} + \frac{\partial \rho}{\partial t} = 0 \quad \text{.......... (2.5)}$$

If $v\frac{\partial \rho}{\partial x}$ is negligible compared to the other terms.

and if $\frac{\partial \rho}{\partial t} = \frac{\partial P}{\partial t}\left(\frac{\partial \rho}{\partial P}\right)_S$ .... (2.6)

where $\frac{\partial \rho}{\partial P} = \rho/E_L$ .... (2.7)

and E_L is the bulk modulus of elasticity of the fluid

then equation (2.5) becomes

$$\frac{\partial v}{\partial x} + \frac{1}{E_L}\frac{\partial P}{\partial t} = 0 \quad \text{.......... (2.8)}$$

The pressure wave moves with the velocity of sound in the fluid, which can be expressed as

$$a^2 = gcE_L/\rho \quad \ldots\ldots\ldots\ldots\ldots\ldots\ldots\ldots\ldots\ldots \quad (2.9)$$

Substituting, the continuity equation becomes

$$\frac{\partial v}{\partial x} + \frac{gc}{a^2\rho}\frac{\partial P}{\partial t} = 0 \quad \ldots\ldots\ldots\ldots\ldots\ldots\ldots\ldots\ldots\ldots \quad (2.10)$$

2.1.2 Equation of motion - force balance

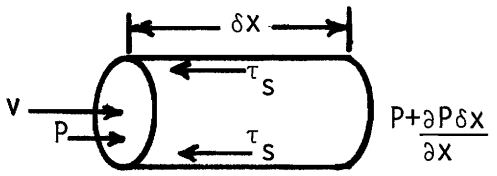

Figure 2.2 Forces acting on fluid in a pipe segment

$$\Sigma F_x = -\frac{\pi D^2}{4}\frac{\partial P}{\partial x}\delta x - \tau_s \pi D \delta x - \frac{\partial z}{\partial x}\delta x \frac{\rho g}{gc}\frac{\pi D^2}{4} \quad \ldots\ldots\ldots\ldots \quad (2.11)$$

$$\frac{MA}{gc} = \frac{\pi D^2}{4}\frac{\rho \delta x}{gc}\left(\frac{\partial v}{\partial t} + v\frac{\partial v}{\partial x}\right) \quad \ldots\ldots\ldots\ldots\ldots\ldots\ldots \quad (2.12)$$

Since $\Sigma F_x = \frac{MA}{gc}$ and $v\frac{\partial v}{\partial x}$ is small compared to $\frac{\partial v}{\partial t}$ and

$$\tau_s = \frac{fv|v|\rho}{2gc} \quad \ldots\ldots\ldots\ldots\ldots\ldots\ldots\ldots\ldots\ldots \quad (2.13)$$

which is essentially a definition of the Fanning friction factor, the force balance becomes

$$\frac{\partial v}{\partial t} + \frac{2fv|v|}{D} + \frac{gc}{\rho}\frac{\partial P}{\partial x} + g\frac{\partial z}{\partial x} = 0 \quad \ldots\ldots\ldots\ldots\ldots \quad (2.14)$$

2.1.3 Simultaneous solution of the continuity and force balance equations

To place the equations in a form, suitable for simultaneous solution, we can multiply equation (2.10) by an unknown multiplier, λ, and add the resulting expression to equation (2.14). We then have

$$\frac{\partial v}{\partial t} + \lambda\frac{\partial v}{\partial x} + \frac{g c \lambda}{a^{2}\rho}\left(\frac{\partial P}{\partial t} + \frac{a^{2}}{\lambda}\frac{\partial P}{\partial x}\right) + g\frac{\partial z}{\partial x} + \frac{2fv|v|}{D} = 0 \quad \ldots\ldots (2.15)$$

When a dependent variable such as $v = f(t,x)$ is differentiated with respect to one variable the chain rule gives

$$\frac{dv}{dt} = \frac{\partial v}{\partial t} + \frac{\partial v}{\partial x}\cdot\frac{dx}{dt} \quad \ldots\ldots (2.16)$$

Thus if $\lambda = \frac{dx}{dt}$ $\ldots\ldots (2.17)$

and $\frac{a^{2}}{\lambda} = \frac{dx}{dt}$ $\ldots\ldots (2.18)$

then equation (2.15) becomes

$$\frac{dv}{dt} + \frac{g c \lambda}{a^{2}\rho}\frac{dP}{dt} + g\frac{dz}{dx} + \frac{2fv|v|}{D} = 0 \quad \ldots\ldots (2.19)$$

and $\lambda = \pm a = \frac{dx}{dt}$ $\ldots\ldots (2.20)$

We then have the following sets of equations for solution:

$$\lambda = +a = \frac{dx}{dt} \quad \ldots\ldots (2.21)$$

$$\frac{dv}{dt} + \frac{g c}{a\rho}\frac{dP}{dt} + g\frac{dz}{dx} + \frac{2fv|v|}{D} = 0 \quad \ldots\ldots (2.22)$$

$$\lambda = -a = \frac{dx}{dt} \quad \ldots\ldots\ldots\ldots\ldots\ldots\ldots\ldots\ldots\ldots\ldots\ldots \quad (2.23)$$

$$\frac{dv}{dt} - \frac{gc}{a\rho}\frac{dP}{dt} + \frac{gdz}{dx} + \frac{2fv|v|}{D} = 0 \quad \ldots\ldots\ldots\ldots\ldots\ldots \quad (2.24)$$

Equations (2.21 - 2.24) are the equations to be used to build a solution of the pressure wave equation at particular values of x and t. The characteristic lines are trajectories in the x-t plane given by equations (2.21 and 2.23), and on these trajectories equations (2.22 and 2.24) are valid respectively.

2.1.4 Finite difference approximations

Since we will assume that the velocity of sound "a" remains constant equations (2.21 and 2.23) plot as straight lines on a t-x plot as shown in figure 2.3.

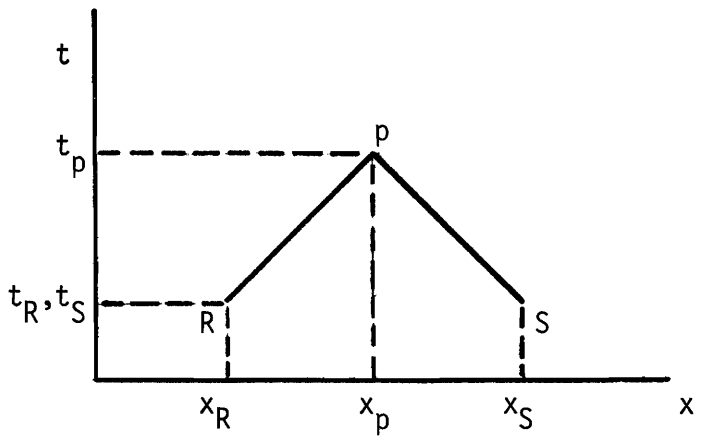

Figure 2.3 Equations (2.21 and 2.23) in the t-x plane

Equations (2.22 and 2.24) can be expressed in finite difference form to solve for conditions at p at a time t_p, using conditions at points R and S at time t_R or t_S. We define the time interval as Δt.

i.e. $\Delta t = (t_p - t_R) = (t_p - t_S)$ ..... (2.25)

The finite difference equations are:

$$x_p - x_R = a\Delta t \quad \text{..... (2.26)}$$

$$v_p - v_R + \frac{gc}{a\rho}(P_p - P_R) + g\left(\frac{dz}{dx}\right)\Delta t + \left(\frac{2fv|v|}{D}\right)_R \Delta t = 0 \quad \text{..... (2.27)}$$

$$x_p - x_S = -a\Delta t \quad \text{..... (2.28)}$$

$$v_p - v_S - \frac{gc}{a\rho}(P_p - P_S) + g\left(\frac{dz}{dx}\right)\Delta t + \left(\frac{2fv|v|}{D}\right)_S \Delta t = 0 \quad \text{..... (2.29)}$$

In order that a solution is always made for the same particular locations within the pipe, it is necessary to calculate P and v at positions lying between the "stations" as shown in figure 2.4.

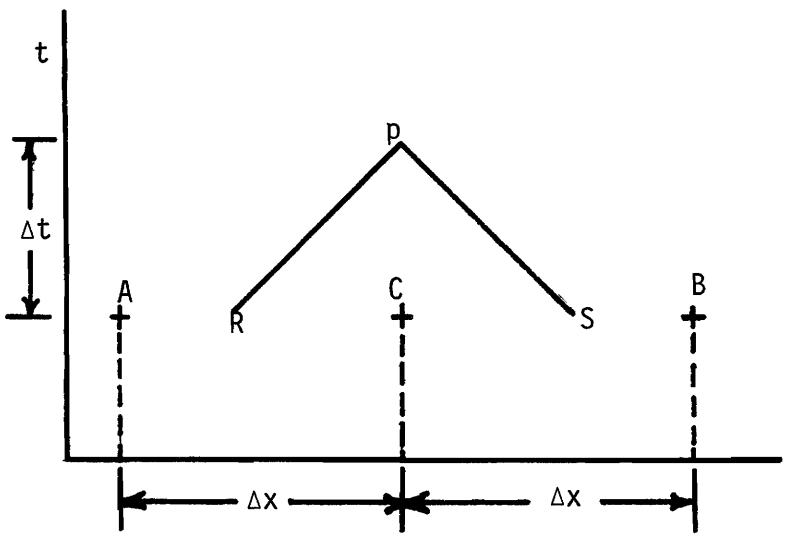

Figure 2.4 "Stations"and interpolation points in the x-t plane

Points A, B, and C are the "stations" in the system for which we wish to know the velocity and pressure at various time intervals. From points A, B, and C the conditions at points R and S, at the same time can be obtained by linear interpolation. Then the conditions at point p can be determined after the time interval Δt, from the interpolated conditions at points R and S, using equations (2.27 and 2.29).
The linear interpolation equations for points R and S are as follows:

$$v_R = v_C + \frac{\Delta t a}{\Delta x} (v_A - v_C) \quad \ldots\ldots\ldots\ldots\ldots\ldots\ldots \quad (2.30)$$

$$P_R = P_C + \frac{\Delta t a}{\Delta x} (P_A - P_C) \quad \ldots\ldots\ldots\ldots\ldots\ldots\ldots \quad (2.31)$$

$$v_S = v_C + \frac{\Delta t a}{\Delta x} (v_B - v_C) \quad \ldots\ldots\ldots\ldots\ldots\ldots\ldots \quad (2.32)$$

$$P_S = P_C + \frac{\Delta t a}{\Delta x} (P_B - P_C) \quad \ldots\ldots\ldots\ldots\ldots\ldots\ldots \quad (2.33)$$

where $\Delta x = (x_A - x_C) = (x_C - x_B)$ $\ldots\ldots\ldots\ldots\ldots\ldots\ldots$ (2.34)

Equations (2.26-2.33) are the general equations to be used for any system. The next section describes the modifications of the equations as they were applied to the pipeline system in this study.

2.1.5 Equations describing the experimental system under study

The particular equations to be used at any station in the experimental system depend upon several factors. Stations which are at either end of the pipeline have boundary conditions associated with them. Interior

stations have the particular problem that $\frac{dz}{dx}$ may be 0, -1, or both over a particular span of the pipeline.

a) Equations used at the head tank outlet

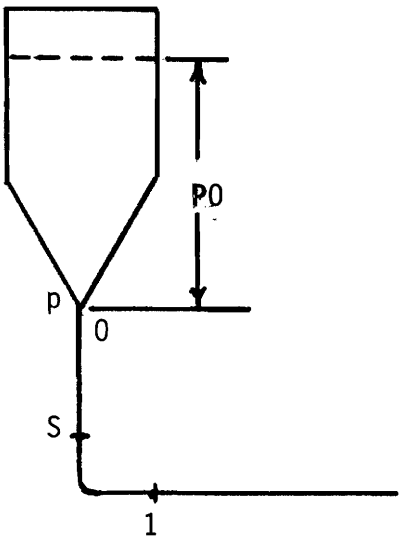

Figure 2.5 Schematic diagram of upstream end of the experimental system

Figure 2.5 shows that portion of the system under consideration. The pipeline is divided into ten equal lengths and the distance from point 0 to point 1 is one tenth of the pipeline length. Point S lies halfway between points 0 and 1. The boundary condition at station 0 is

$$P_p = P0 = \text{constant} \quad \ldots\ldots\ldots\ldots\ldots\ldots\ldots\ldots \quad (2.35)$$

since the head will be maintained very nearly constant in the tank. Equation (2.29) is used to calculate the velocity from conditions at point S in the previous time interval.

Thus

$$v_p = v_S + \frac{gc}{a\rho}(P_p - P_S) + g\Delta t - \left(\frac{2fv|v|}{D}\right)_S \Delta t \quad \ldots\ldots\ldots \quad (2.36)$$

since $\frac{dz}{dx} = -1$ in the segment 0-S on the diagram.

b) Equations used at point 1 in the system

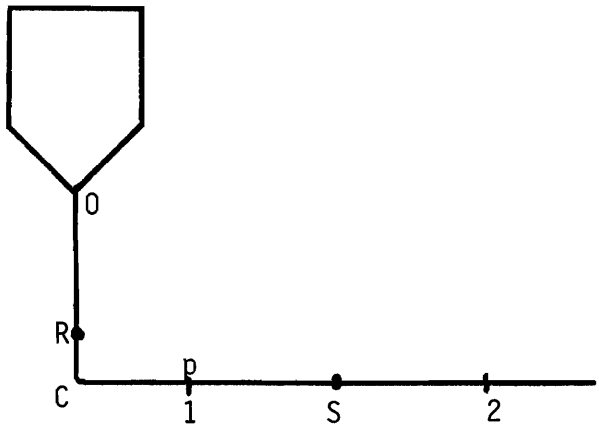

Figure 2.6 Schematic diagram of section of pipeline containing point 1

Since the segment of the pipeline R-1 has $\frac{dz}{dx}$ = 0 and -1, it must be divided into two parts, R-C with $\frac{dz}{dx}$ = -1, and C-1 with $\frac{dz}{dx}$ = 0.
Equation (2.27) becomes

$$v_p - v_R + \frac{gc}{a\rho}(P_p - P_R) - g(t_C - t_R) + \left(\frac{2fv|v|}{D}\right)_R (t_p - t_R) = 0 \quad \ldots\ldots (2.37)$$

Since the line is totally horizontal from 1-S, $\frac{dz}{dx}$ = 0 and equation(2.29) becomes

$$v_p - v_S - \frac{gc}{a\rho}(P_p - P_S) + \left(\frac{2fv|v|}{D}\right)_S (t_p - t_S) = 0 \quad \ldots\ldots\ldots\ldots\ldots (2.38)$$

Simultaneous solution of equations (2.37 and 2.38) provides the equations for station 1. They are the following:

$$P_p = \frac{P_R + P_S}{2} + \frac{a\rho}{gc}\frac{(v_R - v_S)}{2} + \frac{a\rho g}{gc}\frac{(t_C - t_R)}{2} \quad \ldots\ldots\ldots\ldots\ldots\ldots (2.39)$$

$$v_p = \frac{v_S + v_R}{2} + \frac{gc}{a\rho}\frac{(P_R - P_S)}{2} + g\frac{(t_C - t_R)}{2} - \left(\frac{2fv|v|}{D}\right) Av\Delta t \quad \ldots\ldots\ldots\ldots (2.40)$$

It should be noted that $(t_C - t_R)$ can be expressed as $\frac{XCR}{a}$ where XCR is the distance between points R and C.

c) Equations to be used at stations 2-9 in the system

Since these stations all lie in the horizontal portion of the pipeline, equations(2.27 and 2.29) are solved simultaneously with $\frac{dz}{dx} = 0$ to provide the necessary expressions:

$$P_p = \frac{P_R+P_S}{2} + \frac{a\rho}{gc}\frac{(v_R-v_S)}{2} \quad \ldots\ldots\ldots\ldots\ldots\ldots\ldots \quad (2.41)$$

$$v_p = \frac{v_S+v_R}{2} + \frac{gc}{a\rho}\frac{(P_R-P_S)}{2} - \left(\frac{2fv|v|}{D}\right)_{Av}\Delta t \quad \ldots\ldots\ldots\ldots \quad (2.42)$$

d) Equations to be used at the control valve (station 10)

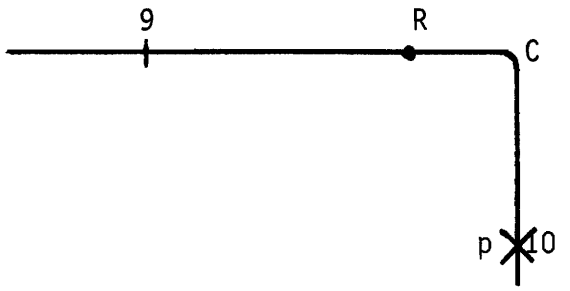

Figure 2.7 Schematic diagram of downstream end of pipeline

Figure 2.7 shows the downstream portion of the pipeline containing the control valve. The segment of the line C-10 has $\frac{dz}{dx} = -1$.
Equation (2.27) becomes

$$v_p-v_R + \frac{gc}{a\rho}(P_p-P_R) - g(t_p-t_C) + \left(\frac{2fv|v|}{D}\right)_R\Delta t = 0 \quad \ldots\ldots \quad (2.43)$$

The boundary condition at the valve is the valve flow equation

$$\frac{v_p}{v_o} = \tau\sqrt{\frac{\Delta P_p}{\Delta P_o}} \quad \ldots\ldots\ldots\ldots\ldots\ldots\ldots\ldots\ldots\ldots (2.44)$$

which relates the velocity at any time, v_p, to the initial steady-state velocity v_o. τ in equation (2.44) is the ratio CV/CVO where:

CV is the valve coefficient and is a function of valve position.

CVO is the valve coefficient corresponding to the initial steady-state flowrate.

ΔP_o is the steady-state pressure drop across the valve and ΔP_p is the pressure drop across the valve corresponding to the flowrate with velocity v_p.

Equations (2.43 and 2.44) are solved simultaneously to obtain the necessary equations.

$$v_p = \frac{-1 \pm \sqrt{1 + \frac{4gcP_o}{a\rho v_o^2\tau^2}\left(v_R + \frac{gcP_R}{a\rho} + g(t_p - t_C) - \left(\frac{2fv|v|}{D}\right)_R \Delta t\right)}}{\frac{2gcP_o}{a\rho v_o^2\tau^2}} \quad \ldots (2.45)$$

$$P_p = P_o(v_p/v_o\tau)^2 \quad \ldots\ldots\ldots\ldots\ldots\ldots\ldots\ldots\ldots\ldots (2.46)$$

Again it should be noted that $(t_p - t_C)$ can be expressed as $\frac{XPC}{a}$ where XPC is the distance from point C to point 10.

It becomes obvious that the calculations at this point are based on

known steady-state conditions, before any disturbance is made through valve motion. The pressure drop across the valve is simply equal to the upstream pressure at the valve, since the line is open to atmospheric pressure downstream of the valve. The next section describes the calculation of the steady-state conditions in the simulation.

2.1.6 Steady-state simulation

In order to begin the simulation of a pressure wave caused by a change in flowrate, it is first necessary to have a steady-state value of the pressure and velocity at the characteristic points in the system. Since the velocity is known and is constant throughout the system at steady-state, the pressure at any point along the line can be calculated from the mechanical energy balance:

$$\frac{P_2-P_1}{\rho} + \frac{U_{b2}^2}{2gc} - \frac{U_{b1}^2}{2gc} + \frac{gz_2}{gc} - \frac{gz_1}{gc} = -W_s - lw_f \quad \ldots\ldots\ldots \quad (2.47)$$

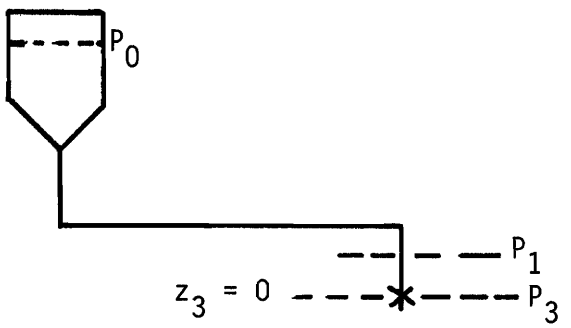

Figure 2.8 Schematic diagram of system

The following simplifications can be made with reference to Figure 2.8:

a) $P_3 = P_0 = 0$ psig

b) $U_{b0} \simeq 0$ ft/sec.

c) $W_s = 0$

d) $lw_f = \frac{2fU_b^2L}{gcD}$

Applying these simplifications to equation(2.47) yields

$$U_{b3}^2 = \frac{-g(z_3-z_0)}{\left(\frac{2fL_3}{D} + \frac{1}{2}\right)} \quad \text{..... (2.48)}$$

where L_3 is the overall equivalent length of the pipeline.

If we apply equation(2.47) to the system at any point P_1, and substitute the expression for the bulk velocity (equation 2.48), since the velocity is constant at any point, the resulting equation is:

$$P_1 = \frac{\rho g}{gc}(z_0-z_1) - \frac{\rho g}{gc}(z_0-z_3)\frac{(D + 4fL_1)}{D + 4fL_3} \quad \text{..... (2.49)}$$

where L_1 is the equivalent length to any position in the line (point 1).

Elevations are measured from a datum at the valve.

The overall equivalent length can be calculated for any velocity using equation (2.48).

Since it is necessary to work in terms of absolute length rather than the equivalent length, an expression of the form, $fL_1 = F_cL$, is more convenient. L is the physical length of the pipeline to the point in question. F_c is a modified friction factor, which has the effect of distributing the friction associated with the elbows over the entire

length of the system. It is the ratio of the equivalent length to the valve divided by the actual length to the valve, multiplied by the normal Fanning friction factor. Experimentally the equivalent length to the valve was found to be 345 feet, and the physical length to the valve from the outlet of the head tank is 229 feet.

Therefore $F_c = f \times 1.51$ ..... (2.50)

and the final equation used for the steady-state simulation is as follows

$$P_1 = \frac{\rho g}{gc}(z_0 - z_1) - \frac{\rho g}{gc}(z_0 - z_3)\frac{(D + 4F_c L)}{D + 4fL_3} \quad \text{..... (2.51)}$$

2.2 Pressure wave velocity

The velocity of a disturbance in a two-phase, solid-liquid system, has been derived using the momentum and continuity relationships and assuming a homogeneous suspension. (Reference 2)

$$C_m = \sqrt{\frac{(c\rho_L + (1-c)\rho_s)}{\rho_s \rho_L} \Big/ \left(\frac{c}{E_s} + \frac{1-c}{E_L} + \frac{D}{E_p t'}\right)} \quad \text{..... (2.52)}$$

ρ_L and ρ_s are the densities of the liquid and solid respectively, and E_s, E_L, and E_p are the bulk moduli of elasticity of the solid, liquid, and pipe respectively.[5] D is the pipe diameter and t' is the pipe thickness. c represents the volume fraction of the solids in the suspension. Equation (2.52) has been experimentally verified for some types of liquid-solid suspensions. (Reference 2)

An attempt was made to measure the velocity of sound in the limestone slurry using a commercial ultrasonic device. This was found to be impossible even at very low concentrations of solids because of the scattering effect of the particles upon the sound waves. Thus for the purposes of the simulation the velocity of sound used was that obtained from equation (2.52).

Footnote: Equation 2.52 is sometimes called the "wave velocity" or "celerity".

2.3 Comments

Some inadequacy of the equations could be expected to occur in the following circumstances:

(a) Rapid pressure changes with Non-Newtonian systems:
The equations of state which are used to obtain f for Non-Newtonian fluids are essentially steady-flow equations, and it is more than likely that wall friction depends upon the time scale of the velocity change as well as the velocity for such substances.

(b) Pipeline startup from rest:
In this case v is a strong function of position within the cross-section of the pipe, and the equations have used an average velocity to compute the wall shear stress. For example, in the case of startup from rest, even a homogeneous fluid must pass through a laminar flow region and the model employs a constant friction factor which is much more nearly reasonable for turbulent flow.

In addition, the application of the equations derived in this section to stratified flow introduces the assumption that mean densities and velocities can be used for the purposes of mathematical modelling.

The experimental program was designed to assess these effects.

CHAPTER 3. DESCRIPTION OF APPARATUS

3.1 General details

The flow circuit is shown schematically in Figure 3.1. The test line is 229 feet long and is constructed from flanged sections of two inch schedule 40 Aluminum pipe. It is fed by gravity flow from a 103 Imperial gallon head tank. The only valve in the test line is the control valve at the outlet

The return line is totally separate from the test line and is also constructed from two inch schedule 40 Aluminum pipe. All valves in the return line are PVC Trans Diaphragm valves. The pump in the return line is a 2X2 Canadian Allis Chalmers SRL rubber lined pump, powered by a 2 H.P., 1800 RPM motor. Because of an excessively worn gland, the water seal was not used in order to avoid dilution of the system. This resulted in a considerable loss of slurry from the system which had to be replaced. However no problem of shaft overheating was encountered. The motor was selected so that the pump would deliver 50 Imperial gallons per minute of a 1.25 specific gravity slurry against a 32 foot head.

The collection tank at the outlet of the test line had a capacity of 115.5 Imperial gallons and was constructed from 12 gauge black iron.

The sections of the pipeline were constructed by welding socket-weld, flat face flanges to the pipe ends. This particular type of flange was used to avoid any changes in diameter of the flow passage. Sections of pipe were aligned using dowel holes in the flanges, and the flanges were then bolted together with ½ inch bolts. A short, removable section was provided in the line for insertion of a magnetic flowmeter.

Figure 3.1 Schematic diagram of the flow circuit

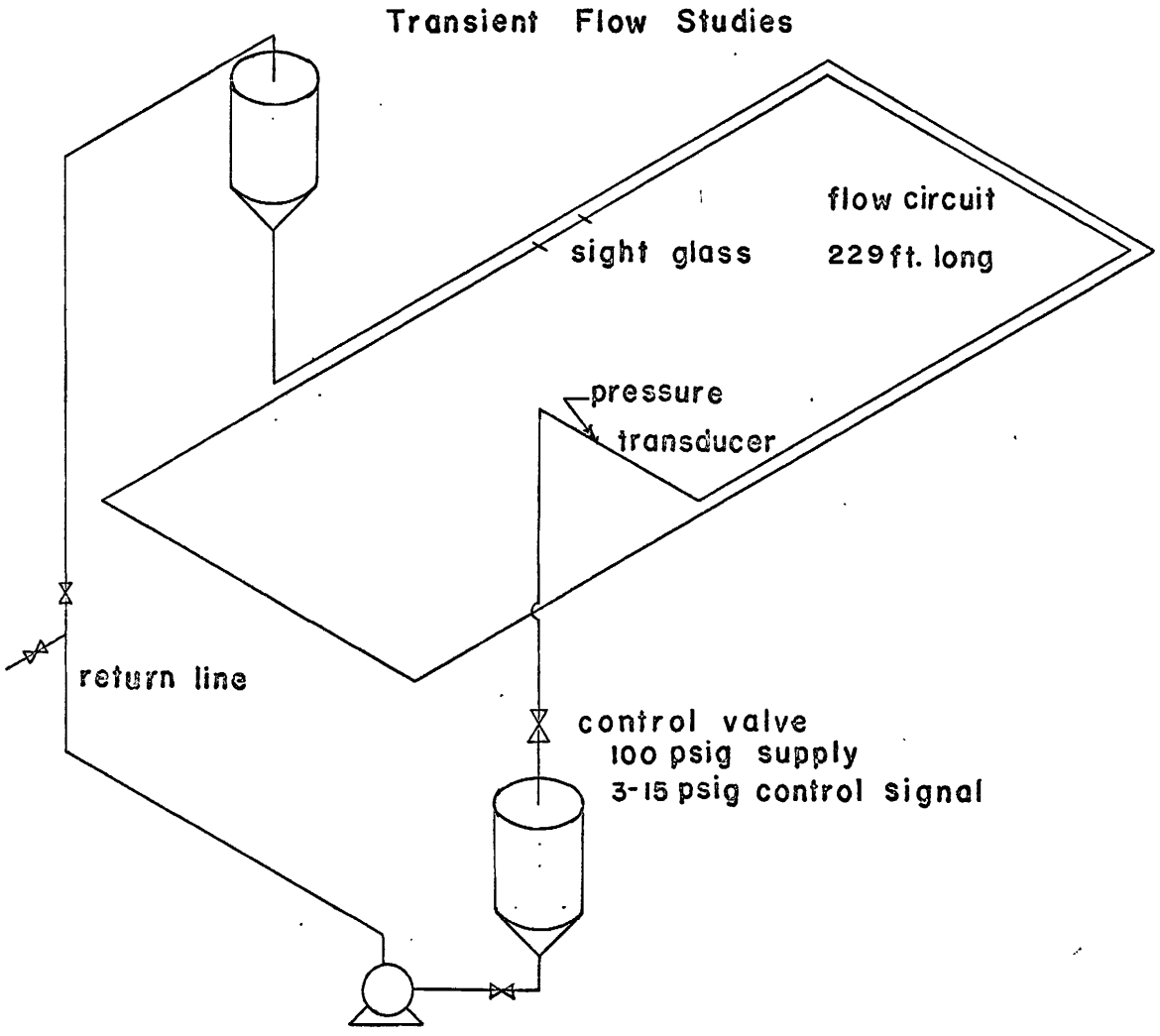
Transient Flow Studies
flow circuit
229 ft. long
sight glass
pressure
transducer
return line
control valve
100 psig supply
3-15 psig control signal

A sightglass approximately 1½ feet long was constructed from Perspex. The inside was machined to the same diameter as the inside of the aluminum pipe - 2.067", also to avoid any abrupt changes in diameter. Through the sightglass the flow during startup was photographed using a Bolex 16mm cine camera.

The entire pipeline was suspended by pipe hangers from the ceiling and was secured using strapping and lag-bolts in any locations which were possible. Securing the line was essential to avoid possible violent vibrations of the line during the passage of the pressure wave.

The vertical elevation from the control valve to the outlet of the head tank is 20.46 feet. An average head of 3 feet is maintained in the head tank, so the overall head is 23.46 feet. From the outlet of the head tank to the horizontal section of the line is a vertical distance of 19.83 feet, and from the horizontal portion to the control valve is a vertical distance of 2.63 feet.

In the test line there is a total of two 45 degree elbows and nine 90 degree elbows. All elbows are schedule 40 long radius elbows.

For the purpose of preventing solids from plugging the vertical section immediately after the head tank, a large rubber stopper was fixed onto a length of pipe for insertion into the outlet of the tank at any time the slurry was to be held in the head tank. Under normal conditions the slurry was held in the bottom tank while the system was not being operated. In addition a steel ball, 1¼ inches in diameter was lowered to the bottom of the vertical section prior to pumping the slurry to the head tank. Withdrawal of this ball just before the run assisted in maintaining the solids in suspension. At high concentrations of solids this problem is not too serious as the rate of settling is fairly slow.

The steel ball was also used to determine the level of the slurry in the vertical leg. This was necessary when the system was being drained in preparation for a startup run, to insure that the vertical leg contained no slurry. It was essential that the system was drained just to the horizontal portion of the pipeline and no further, to avoid trapping air bubbles in the line.

A similiar rubber stopper plug was used in the bottom tank when the system was shut down to avoid plugging the feed line to the pump.

In addition, a rubber stopper with a moveable plunger was inserted into the outlet of the pipeline prior to a startup. The control valve was opened and the plunger inserted up the short vertical section leading to the valve. This was done to loosen any solid plug that may have formed during shutdown.

3.2 Flow measurement

Flow rates in the system were measured by timing a six inch drop in level in the head tank. Using a pressure tap immediately upstream of the control valve, the pressure drop over the valve could be measured as a function of water flowrate. This data was then used to determine the valve coefficients of discharge as a function of valve stem position.

3.3 Pressure measurement and recording

The requirements for measuring transient pressures are a very fast response time and high resolution. In the case under study it is also

necessary to produce a minimum disturbance in the flow with the measuring device. These requirements were met by the Kistler Quartz pressure transducer (Model 601A1). The pressure range of the instrument is 0 - 3000 psia with resolution being essentially infinite (limited only by noise in the signal conditioning equipment). The resonant frequency is 250 KHz and the transducer is only ¼ inch in diameter. In general this type of transducer converts applied pressure to electrical charge signals. They feature high linearity and repeatability over a wide range of pressures and temperatures. The high natural frequency of rigid quartz transducer elements permits measurement of high frequency pressure variations and fast rise-time components of explosion and blast pressures. The transducer element is preloaded to permit measurement of pressures below atmospheric. These transducers are normally restricted to dynamic pressure measurements, but static calibration is readily accomplished through step inputs on a dead-weight gauge tester.

In order to obtain the best frequency response, the transducer was flush mounted in the pipeline five feet upstream of the control valve. Figure 3.2 shows the installation details.

The signal conditioning equipment used in conjunction with the transducer is the Kistler model 504A Dial-Gain charge amplifier. This instrument converts the charge signal from the transducer to a voltage output. When the transducer sensitivity dial is set to the charge sensitivity of the transducer (1 Pcb/Psi nominal), output signals will have integral values of Psi/volt as selected by the Range switch. A ground switch is provided which restores amplifier output to zero regardless of the actual pressure on the transducer. In addition

Figure 3.2 Pressure transducer installation details

KISTLER INSTRUMENT CORP. 8989 SHERIDAN DRIVE CLARENCE, N. Y. 14031	DESCRIPTION Installation Instructions	MODEL 601A1/601L1

FIG. 5

INSTALLATION OF STANDARD FLUSH MOUNTED MODEL 105A CONNECTOR ADAPTOR WITH MODEL 601A1 or 601L1 PRESSURE TRANSDUCER

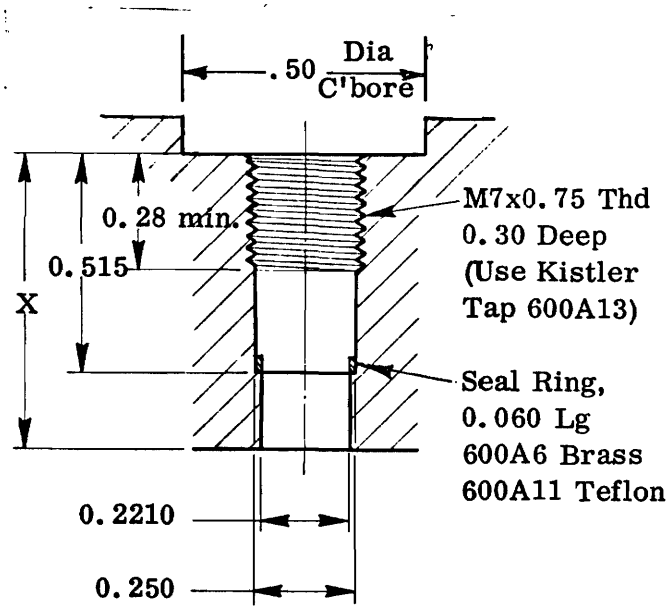

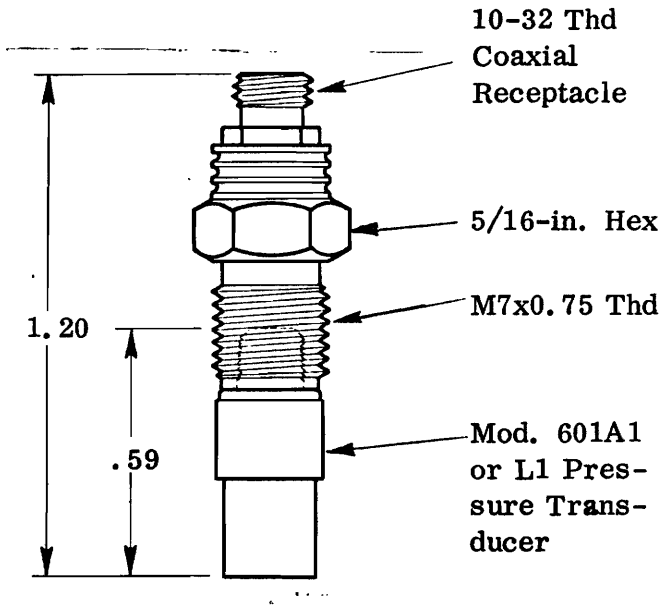

Dim X	0.70 For Flush Mounting
	0.74 For Recessed Mfg

Note: 1. Use 5/16-in. six-point Socket; tighten to 2 lb-ft torque.

APPROVALS	DATE	REVISIONS	DWG. No.
DSGN		A D G	
ENGRG		B E H	
PROD MGR		C 25 F J	Sheet 1 of 2

a calibration circuit is provided with which the operation of the charge amplifier can be checked without the use of the transducer.

The transducer is connected to the charge amplifier by Model 121M low noise cable, a Model 102 adaptor, and Model 131A low noise extension cable.

The output from the charge amplifier is fed to a Model 503 Tektronix oscilloscope, and the trace was photographed using a Model C-27 Tektronix oscilloscope camera. The sweep time used was 0.1 second/cm providing a total sweep time of 1 second. The sweep was triggered by electrical noise generated when switching a solenoid valve, which provides the signal pressure to the control valve positioner.

Pictures of the pressure traces were analyzed under a microscope. One centimeter divisions in the picture from the oscilloscope grid were divided into ten equal divisions using a microscope eyepiece with a grid. This enabled pressure readings at 0.01 second intervals to be obtained from the pressure traces.

3.4 Control valve and operation

The control system installed in the test line consists of a pneumatically driven valve with a positioner. The valve is a 2 inch A4436MT Jamesbury "Double-Seal" Ball valve with N.P.T. screwed ends. The body is of aluminum construction and the ball and stem is of 316 grade Stainless steel. The seats are made of modified Teflon (25% glass fibre fill) and the seals are made of Teflon. The actuator is a Jamesbury ST-50E pneumatic valve actuator requiring a 100 Psi air supply and

producing 50 foot-pounds of torque. The body and cylinder are constructed of aluminum with an epoxy overcoating. The positioner is a Type 400 Moore positioner with a signal pressure range of 3-15 Psig. The air consumption is 0.78 SCFM at 100 Psig and the characteristics are linear. The combined characteristics of the ball valve and this positioner is equal percentage response, which produces equal percentage increments in flow for equal increments in opening or signal.

The control pressure to the positioner is provided by two pressure regulators and a solenoid valve as shown in Figure 3.3. The solenoid valve is used to provide rapid switching from one signal pressure to the other.

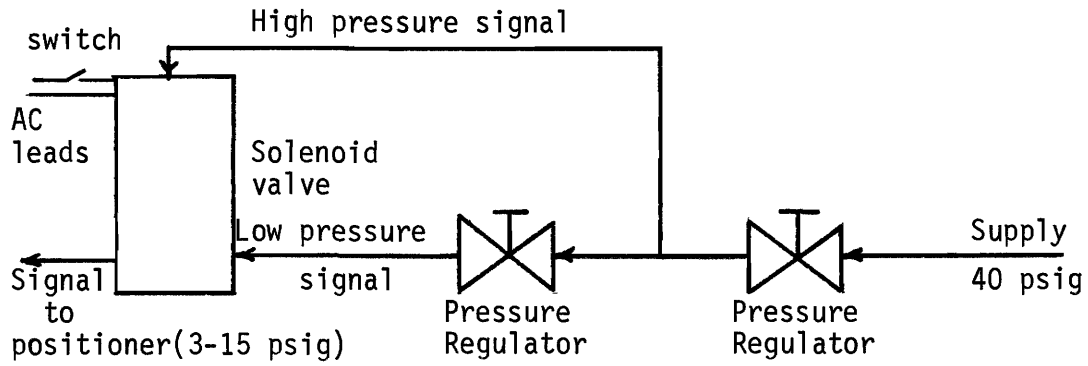

Figure 3.3 Schematic diagram of signal pressure apparatus

Since the actual air consumption rate of the signal pressure line is very small, it is necessary that the signal pressure be always switched from a low pressure to a higher pressure. The reverse operation results in a very slow change in the valve position as the pressure is slowly dissipated. Thus two modes of operation are required. They are:

a) Increasing signal pressure causing the valve to open.

b) Increasing signal pressure causing the valve to close.

To achieve the two modes of operation, it is necessary to reverse the two air supply lines to the actuator. The direction of rotation of the feedback chain on the valve stem extension must also be reversed. The feedback chain is connected to the valve stem and it provides the mechanical feedback to the positioner as the positioner sets the valve position.

The air supply for both the actuator and the signal pressure is supplied from compressed air cylinders, thus avoiding fluctuations in the supply pressure. This method of supply also eliminated the need for air filtering apparatus. The air pressure regulators are Watts Series 16 regulators and the solenoid valve is a Skinner Three-way Type V54 stainless steel valve, operated by 110 volts AC.

CHAPTER 4. PRELIMINARY EXPERIMENTAL WORK

4.1 Determination of valve characteristics

In the computer simulation it is necessary that the relationship between flowrate and pressure drop over the valve be known at any instant (Equation 2.44).

This relationship is of course a function of valve stem position, which is determined by the signal pressure and the direction of valve rotation. The procedure which was employed to determine the desired relationship involved two steps.

a) Valve positions were determined as functions of time and signal pressure, by taking measurements from film records of the opening and closing processes. These results are shown in Figure 4.1.

b) Steady flow measurements using water were used to determine the valve coefficient CV as a function of signal pressure. Since signal pressure determines the valve position Figure 4.2 could be prepared. The steady flow measurements may be seen to substantiate the manufacturer's data for the valve.

Thus, subject to the assumption that the valve coefficient is only a function of the stem position when the stem is moving, the two graphs could be used to give CV as a function of time. This information is used to provide τ in Equation 2.44. The relationship between CV and time was approximated by a series of straight line segments for the purposes of computer calculations.

Figure 4.1 Valve rotation versus Time

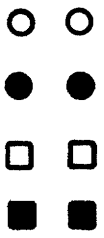

Signal pressure change 3-15 Psig, opening

Signal pressure change 7-10 Psig, opening

Signal pressure change 3-7.7 Psig, closing

Signal pressure change 7-10 Psig, closing

α° indicates the angular rotation of the valve with the reference being zero degrees of rotation when the valve is shut.

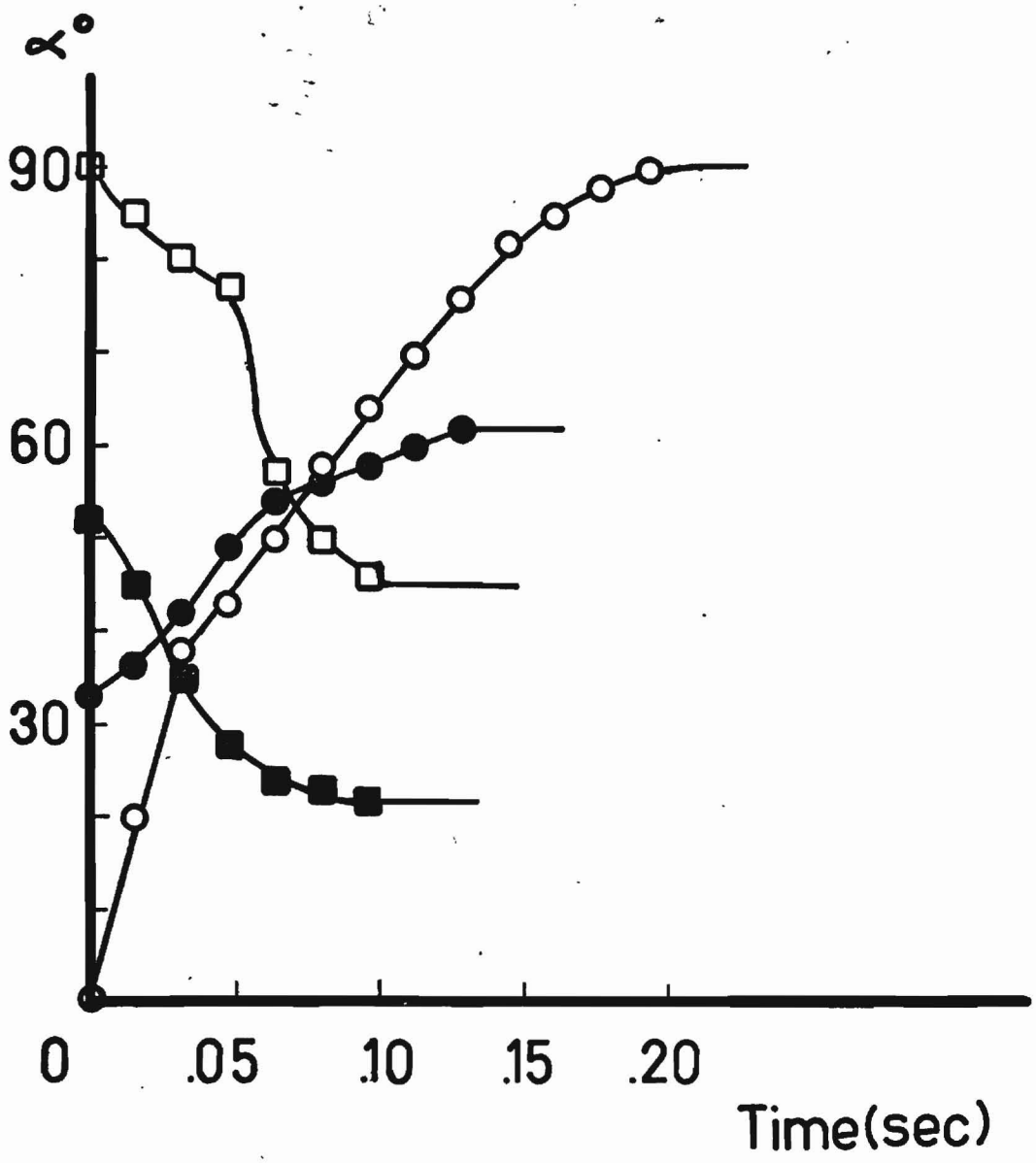
α°
90
60
30
0
.05
.10
.15
.20
Time(sec)

Figure 4.2 Valve coefficient CV (Imperial gallons per minute) versus valve position

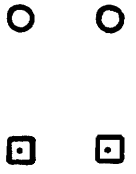

Manufacturer's data

Experimental points

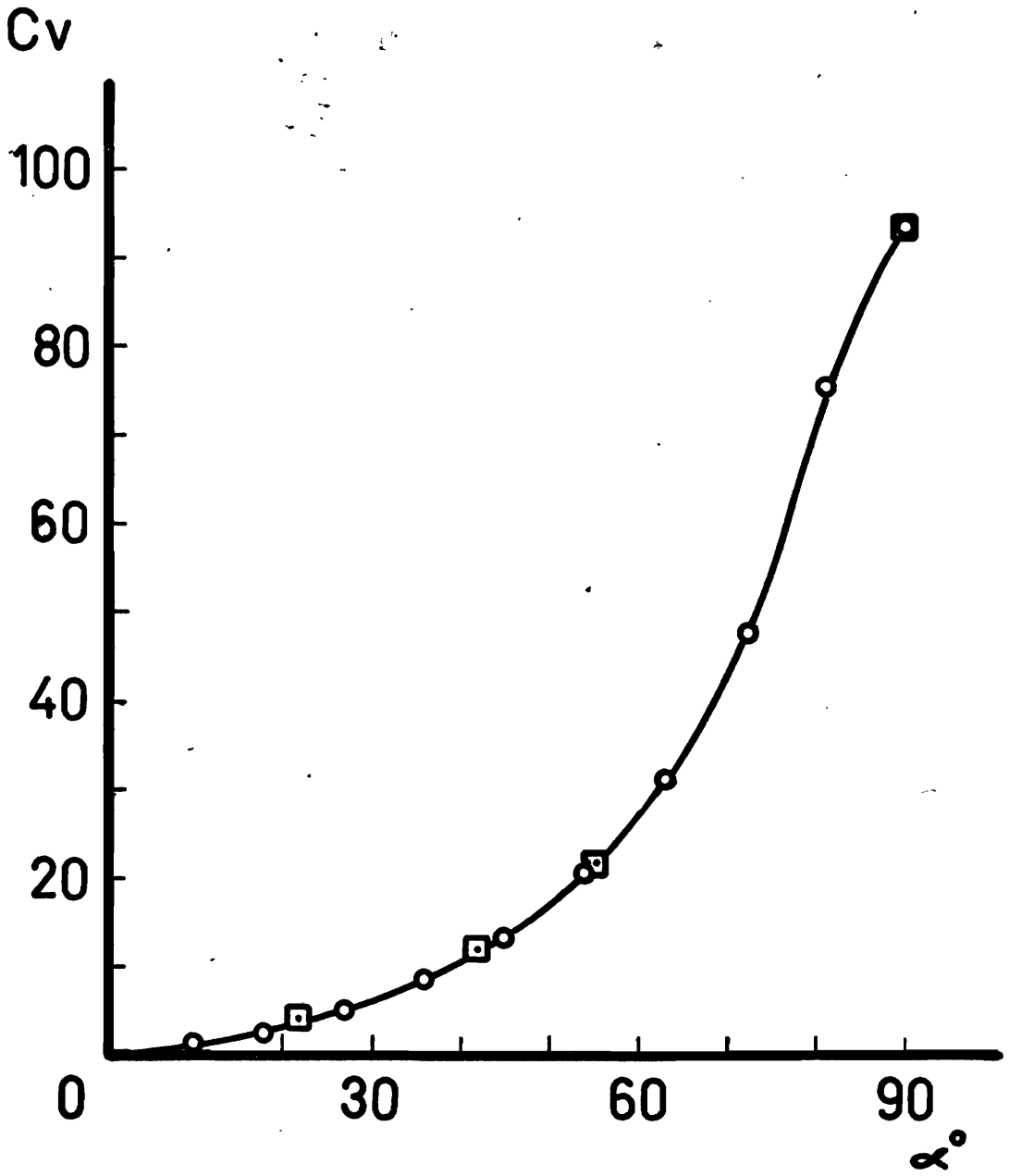
Cv
100
80
60
40
20
0
30
60
90
α°

4.2 Calibration of the pressure transducer and the charge amplifier

The charge amplifier contains a circuit for checking its calibration. A voltage is applied to the "Cal Input" connector and the circuit produces a charge signal input of (1000 X voltage applied) in pico-coulombs. The calibration was checked by setting the time constant switch to "long" and the transducer sensitivity dial to 10.00 Pcb/psi. At each position an input signal (in picocoulombs) equal to ten times the black range marking should produce exactly 1.00 volt output. The output voltages in the various ranges are shown in Table 4.1. Since the amplifier was calibrated at the factory and since a precision voltage supply was not available to provide a stable charge signal, no recal-ibration was attempted. The voltages obtained were very close to one volt in all ranges showing that the amplifier was in proper working order.

TABLE 4.1

Charge amplifier calibration check

Range (psi/volt)	Output (volts)
2	0.94
5	0.98
10	0.98
20	1.0
50	1.0
100	1.0
200	1.0
500	1.05
1000	1.0
2000	0.99

The calibration of the pressure transducer was checked using step inputs on a Dead-weight gauge tester. The factory recommended value for the charge sensitivity is 1.0 Picocoulombs/psi and this was set on the charge sensitivity dial on the charge amplifier. Table 4.2 shows the applied step changes in pressure and those indicated by the transducer.

TABLE 4.2

Pressure transducer calibration check

Applied step change (psi)	Pressure change indicated (psi)
5.00	5.0
10.00	10.0
15.00	15.0
20.00	19.65
25.00	24.9
40.00	39.5
50.00	49.9
100.00	98.8
200.00	200.
500.00	500.

The closeness of the measured pressure changes to the exact values indicated that the charge sensitivity as stated was correct.

4.3 Characterization of limestone

Several tests were conducted to find the size distribution of the limestone used in this study.

A dry screen analysis was made which provided the size distribution in the +325 mesh range. A wet screen analysis and the Andreasen pipette were used to obtain the size distribution in the -325 mesh region. The size distribution of unused limestone and a sample taken from the 35% slurry after pumping is shown in Figure 4.3. It can be seen that very little degradation of the particles occurred during the experimental runs.

From the curves in Figure 4.3, the average particle size can be seen to be 23 microns. Stokes' law predicts a terminal settling velocity of 1.5×10^{-3} ft/sec for particles of this size and density (specific gravity = 2.69). Settling tests were performed on the limestone. This data, when plotted to test the relationship (Equation 4.1), gave a value of V_∞ (by extrapolation) of 1.45×10^{-3} ft/sec, and a value of 9.55 for the exponent n. This high value of n indicates that the suspension was flocculated.

$$\frac{V_s}{V_\infty} = \varepsilon^n = (1-c)^n \quad \ldots\ldots\ldots\ldots\ldots\ldots\ldots\ldots \quad (4.1)$$

The density of the solid limestone was determined by water displacment. A small weighed amount of the limestone was placed in a 100 ml. flask and the flask was filled with water from a burette. Any air trapped in the flask was removed by placing the flask in an ultrasonic generator. The average value for the density of the solid limestone was found to be 2.69 gm/cc.

Figure 4.3 Particle size distribution of limestone

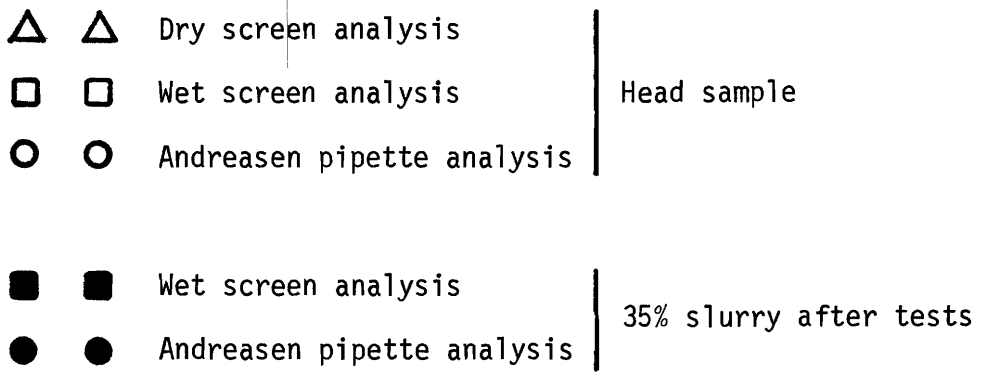

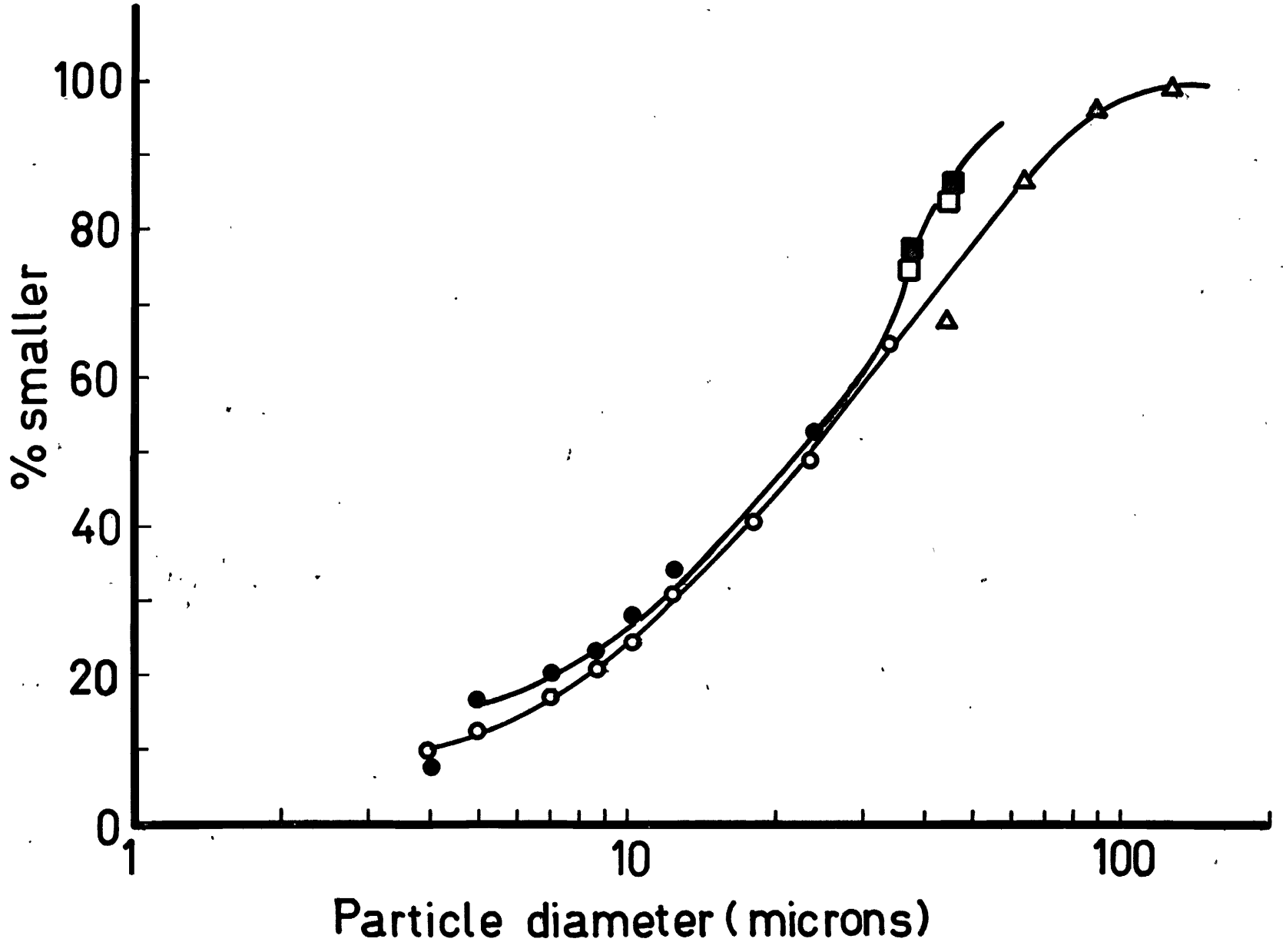
100
80
60
40
20
0
% smaller
1
10
100
Particle diameter (microns)

4.4 Characterization of slurries

The Rheological properties of the slurries were measured using a Brookfield viscometer and a tube viscometer. Experiments were conducted with the Brookfield viscometer using the LV1 spindle in one set of tests and the UL adaptor in a second set. Settling of the suspensions caused severe problems in slurries at concentrations below 30% by volume. Slurries with concentrations above 35% could not be studied adequately. Experiments were conducted using a horizontal tube viscometer with tube diameters of .345, .498, and .615 inches. At velocities low enough to provide laminar flow, settling was again a serious problem with slurries of low concentrations. The data obtained from the three experimental methods is shown in Figure 4.4. From the scatter in the experimental points it can be seen that it is very difficult to obtain reliable data for the rheological properties of the slurries. Experimental data from each method was consistent. However, the data from the different methods did not agree well.

Like most slurries, a Bingham plastic model seemed to be appropriate. Table 4.3 shows the rheological properties estimated from Figure 4.4.

TABLE 4.3

Rheological properties of experimental slurries

Concentration % by vol.	Viscosity, μ_p(cp)	Yield stress, $\tau_y \left(\frac{\text{dynes}}{\text{cm}^2}\right)$
10	1.0	1.0
20	1.0	1.0
30	1.77	3.4
35	3.7	5.2

Figure 4.4 Rheological data for experimental limestone slurries

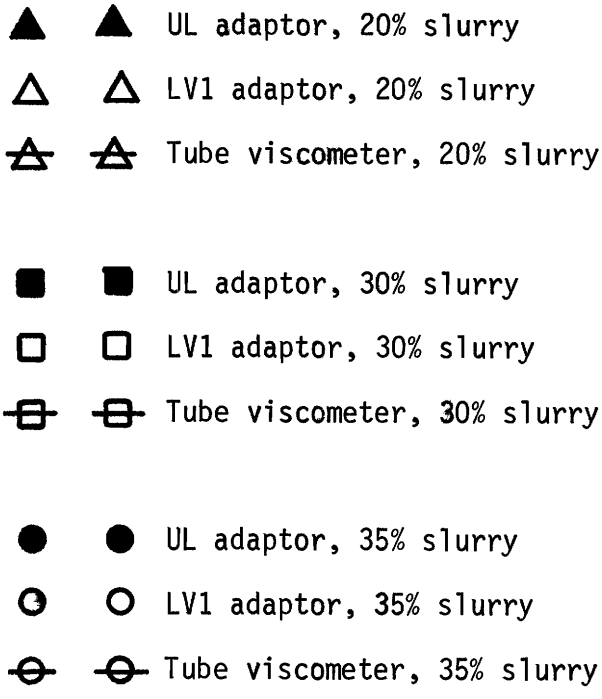

The solid lines were fitted visually as estimations. The slope of the line for the 20% slurry is a minimum value because this slope corresponds to the viscosity of the carrier fluid.

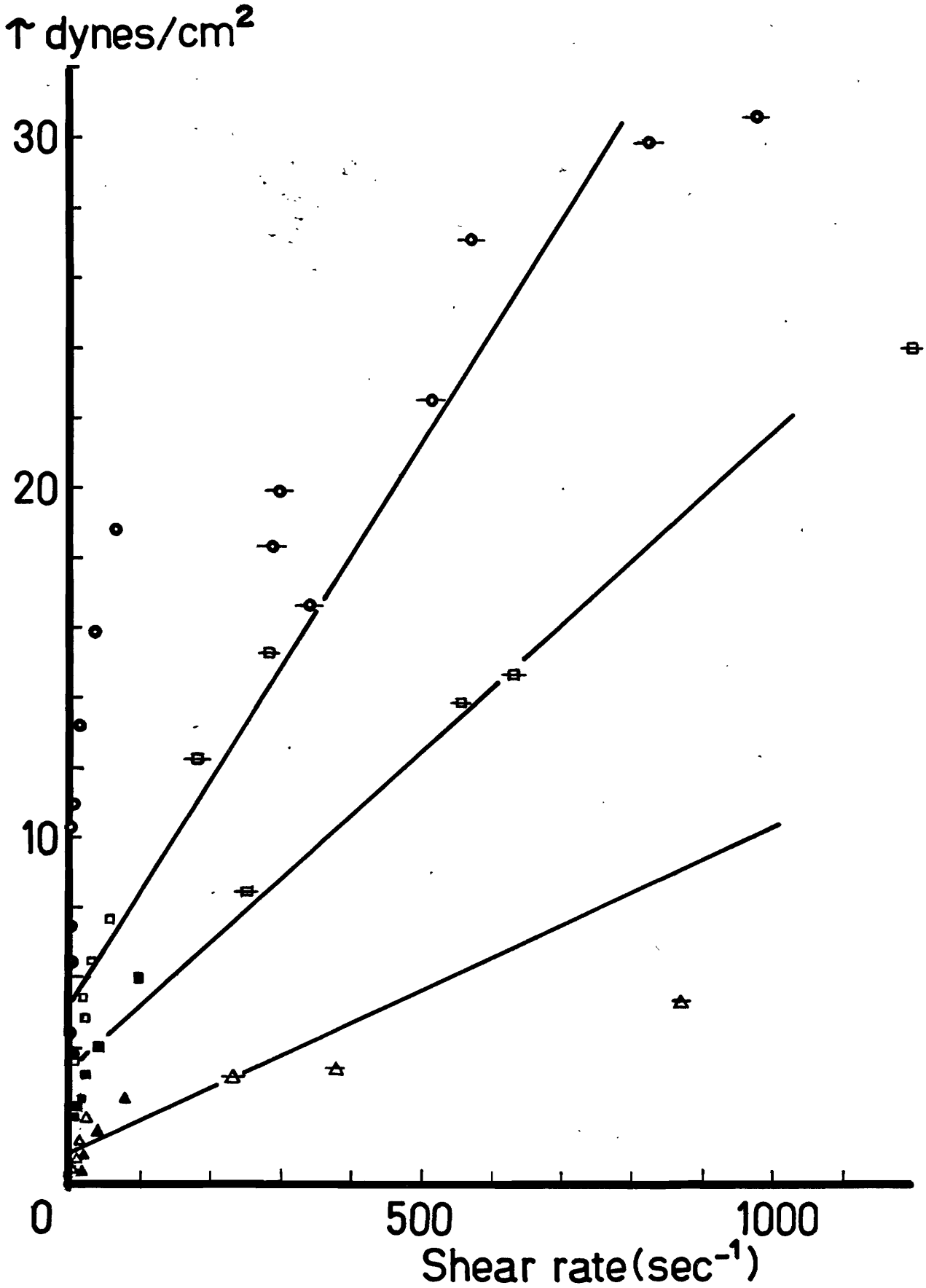
τ dynes/cm²
30
20
10
0
500
1000
Shear rate(sec⁻¹)

CHAPTER 5 EXPERIMENTAL RESULTS AND DISCUSSION

5.1 Water results

Figures 5.1 and 5.2 show the experimentally measured pressure wave and the calculated pressure wave at the pressure transducer for water. It can be seen that the agreement between the simulated and experimental results is good.

The velocity of sound used in the simulation was 3990 feet/second. The friction factors and initial and final steady state conditions are shown on the title page for each figure. The experimental curves were reproducible to a very high degree and all runs were repeated at least once and often several times. The small high frequency fluctuations in the experimental traces are probably the result of vibrational noise in the system. Of general importance is the fact that the experimental traces and the simulation curves have the same shape during the period of valve motion, thus indicating the accuracy of the valve characteristic equations in the simulation.

5.2 Slurry results

Figures 5.3 to 5.10 show the experimental and simulation results for 10%, 20%, 30%, and 35% slurries. As with the water, the results are generally good. A fairly large offset between experimental and simulated curves in the 20%, 30%, and 35% slurries for the case of valve opening (7-10psi control signal) is attributed to a small error in either the initial or final control signal pressure to the valve. Since valve

Figure 5.1 Water results - experimental and simulated pressure curves

ΔP (psi) vs Time (seconds)

Upper: 3-7.7 closing

——— experimental

----- simulation f = .0045

V_i = 6.24 ft/sec

V_f = 3.55 ft/sec

Lower: 7-10 closing

——— experimental

----- simulation f = .0048

V_i = 4.8 ft/sec

V_f = 1.66 ft/sec

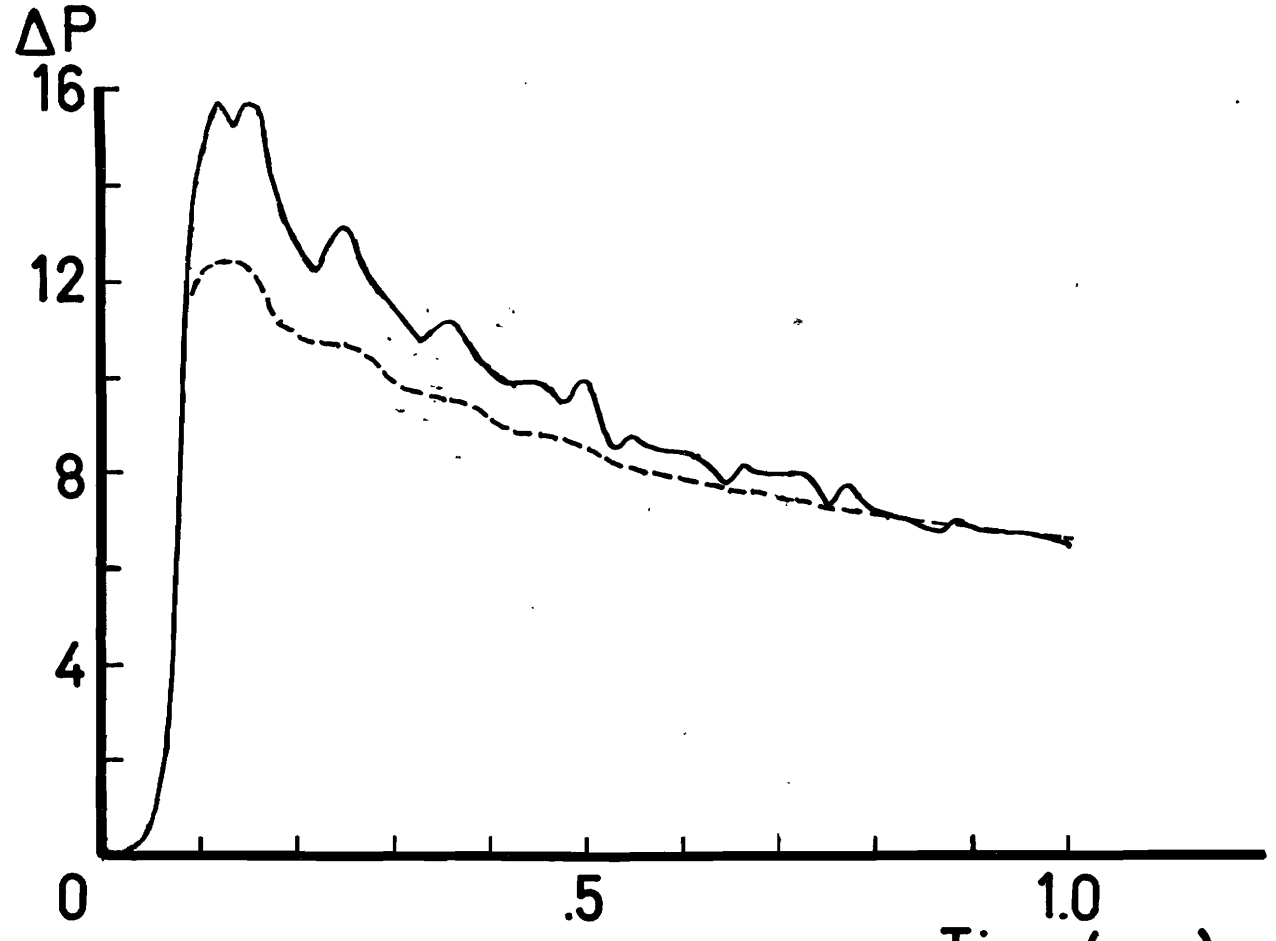
ΔP
16
12
8
4
0
.5
1.0
Time(sec)

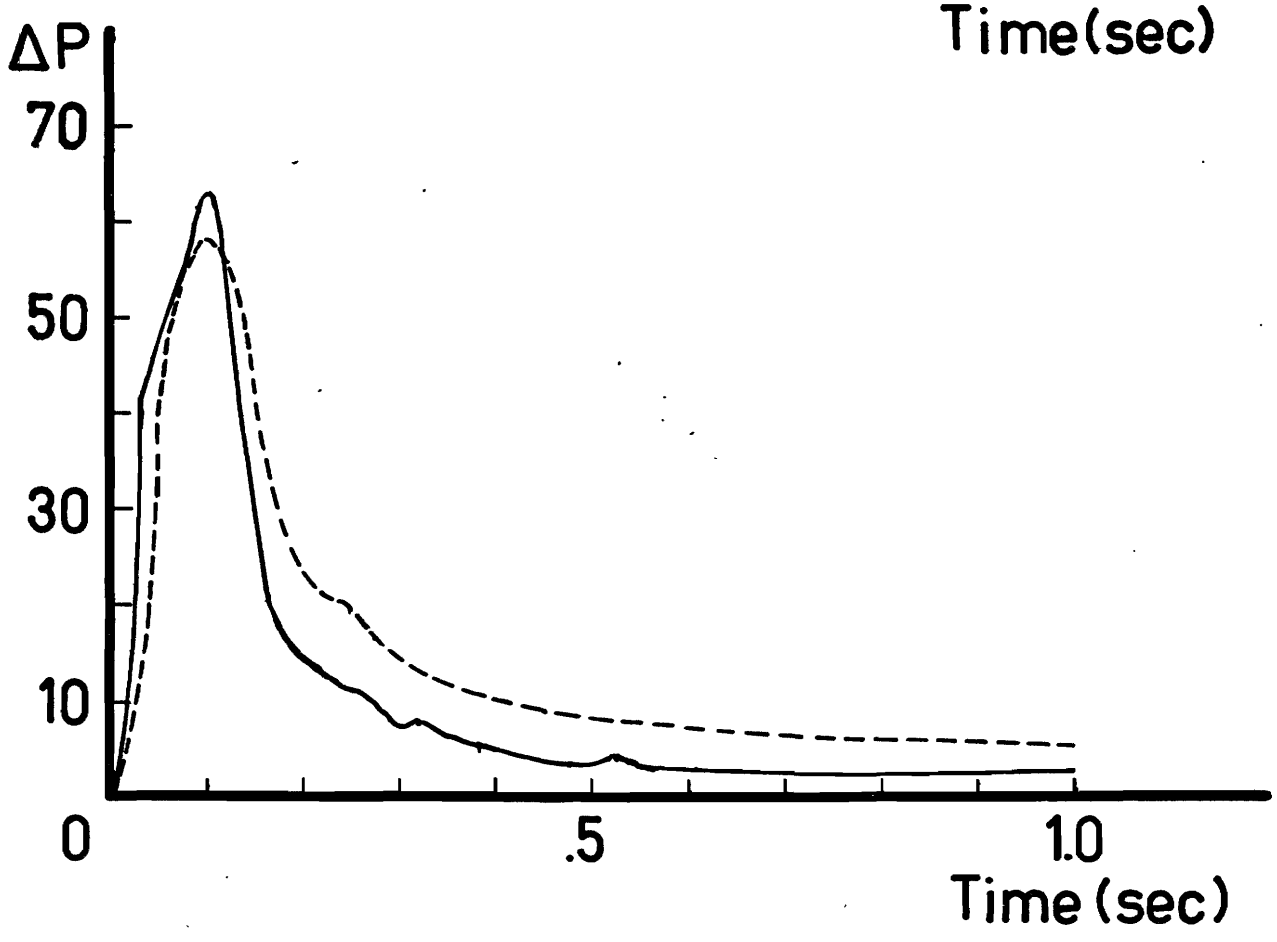
ΔP
70
50
30
10
0
.5
1.0
Time (sec)

Figure 5.2 Water results - experimental and simulated pressure curves

ΔP (psi) vs Time (seconds)

Upper: 3-15 opening

——— experimental

----- simulation f = .0045

V_i = 0 ft/sec

V_f = 6.24 ft/sec

Lower: 7-10 opening

——— experimental

----- simulation f = .0052

V_i = 2.2 ft/sec

V_f = 5.22 ft/sec

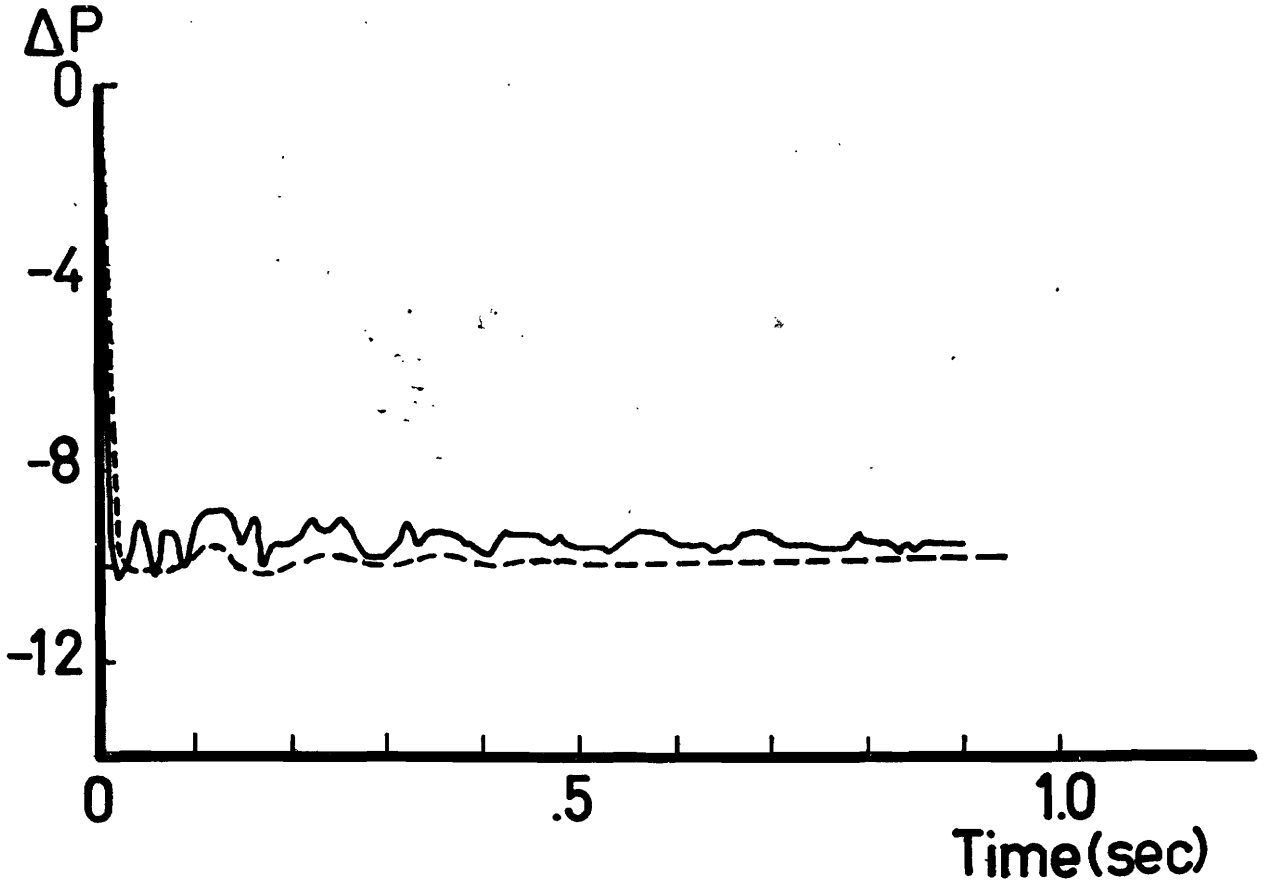
ΔP
0
-4
-8
-12
0
.5
1.0
Time(sec)

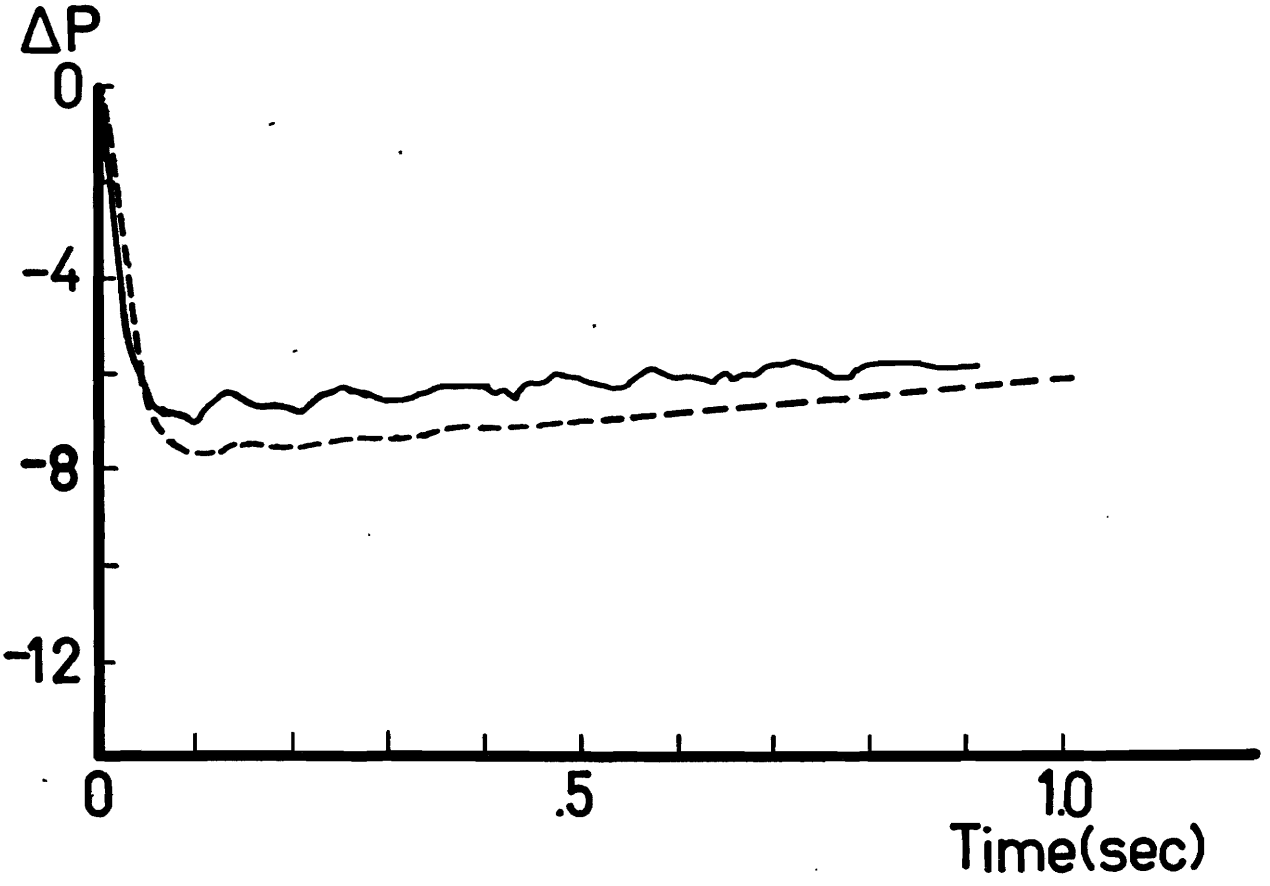
ΔP
0
-4
-8
-12
0
.5
1.0
Time(sec)

Figure 5.3 Slurry results - experimental and simulated pressure curves

ΔP (psi) vs Time (seconds), 10% slurry

Upper: 3-7.7 closing

——— experimental

----- simulation f = .0062

V_i = 5.29 ft/sec

V_f = 3.26 ft/sec

Lower: 7-10 closing

——— experimental

----- simulation f = .0087

V_i = 3.55 ft/sec

V_f = 1.04 ft/sec

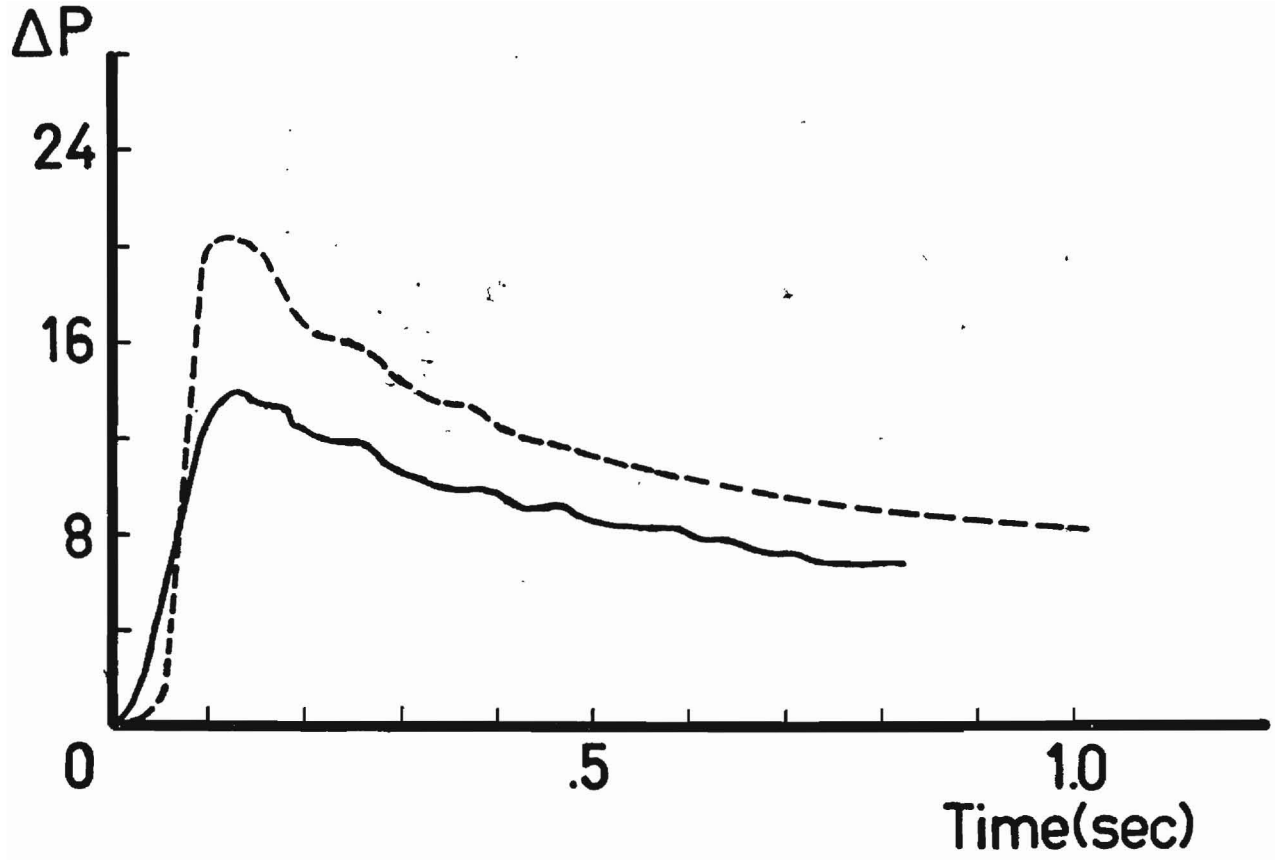
ΔP
24
16
8
0
.5
1.0
Time(sec)

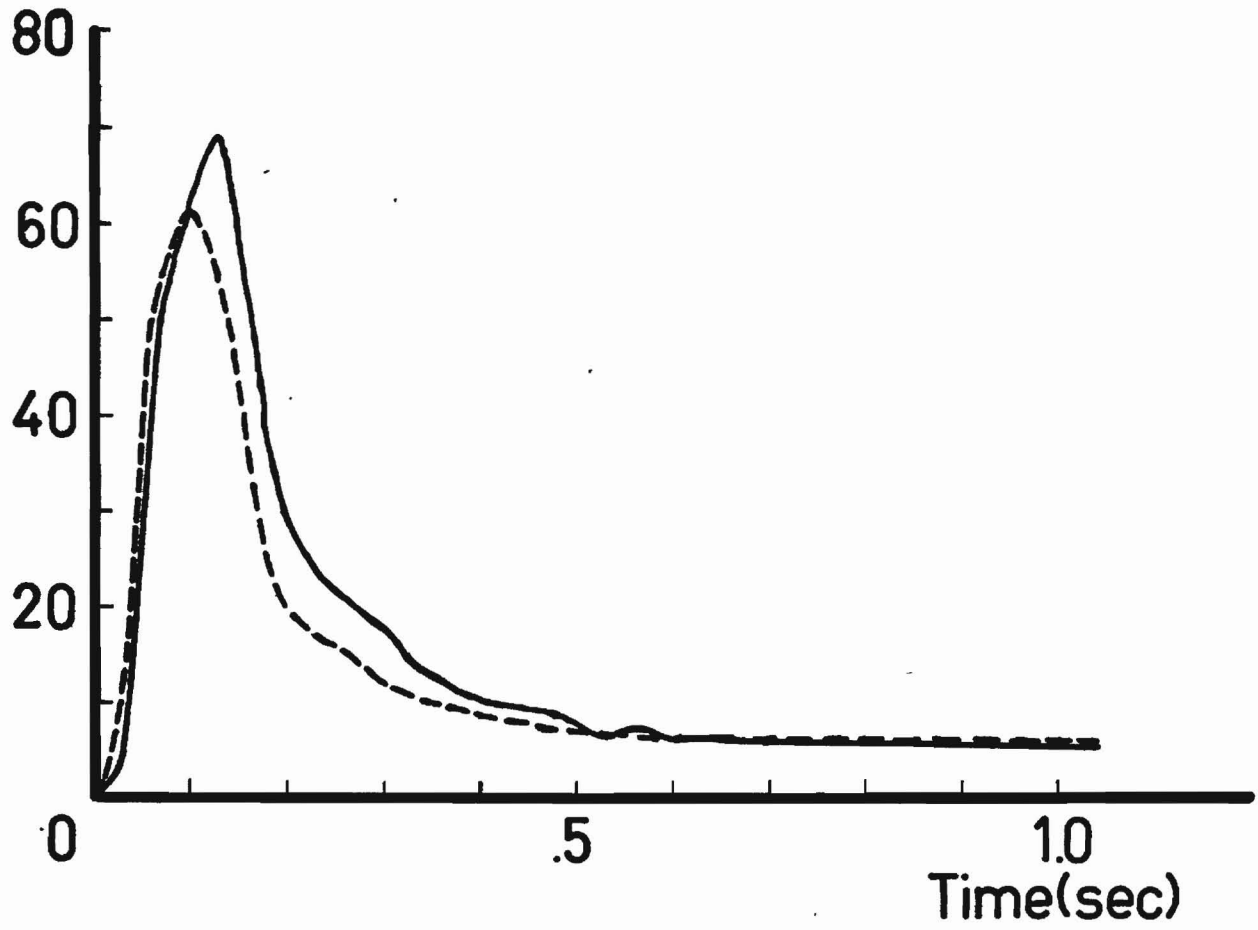
80
60
40
20
0
.5
1.0
Time(sec)

Figure 5.4 Slurry results - experimental and simulated pressure curves

ΔP (psi) vs Time (seconds), 10% slurry

Upper: 3-15 opening

——— experimental

----- simulation f = .0062

V_i = 0.0 ft/sec

V_f = 5.29 ft/sec

Lower: 7-10 opening

——— experimental

----- simulation f = .0080

V_i = 1.71 ft/sec

V_f = 3.93 ft/sec

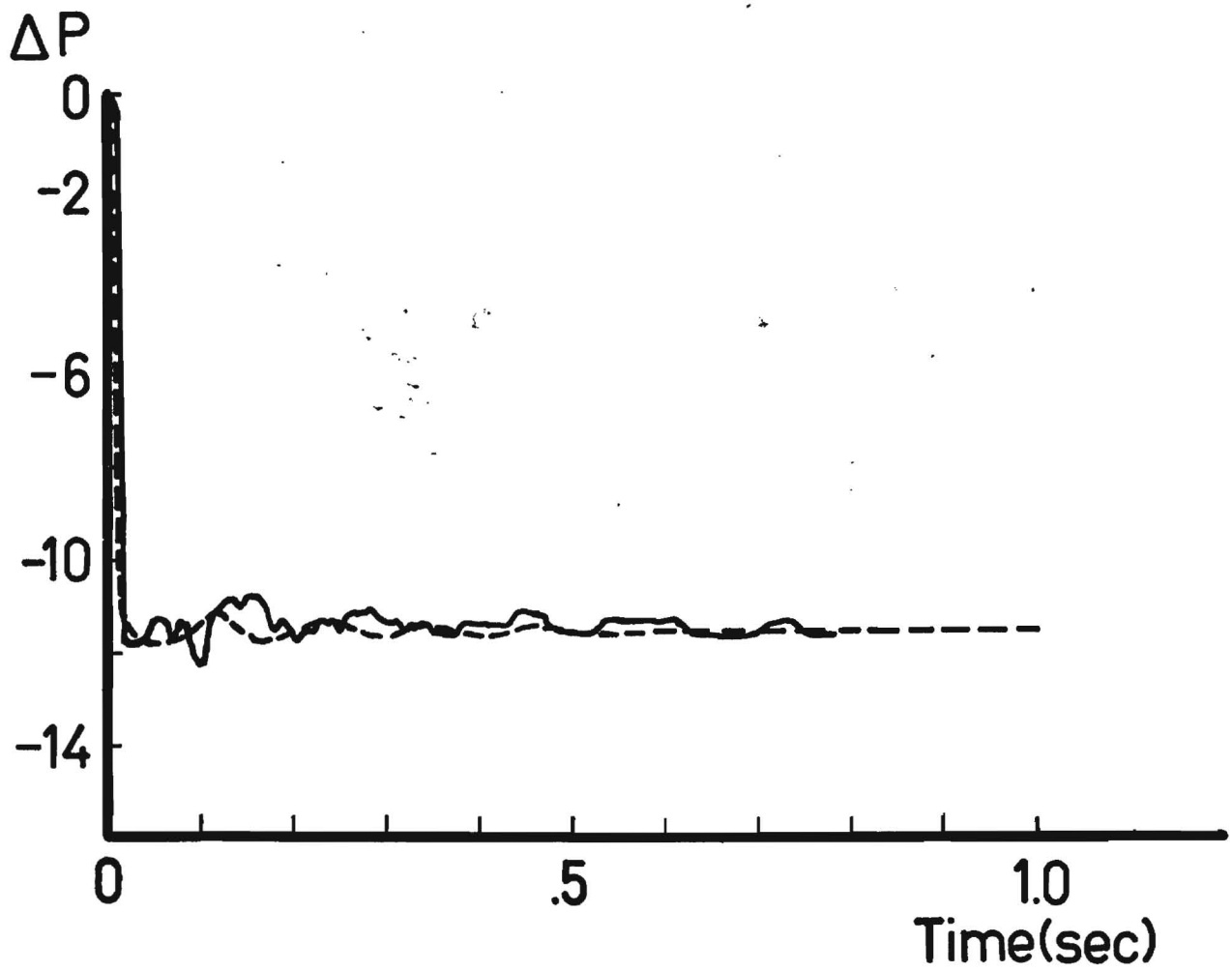
ΔP
0
-2
-6
-10
-14
0
.5
1.0
Time(sec)

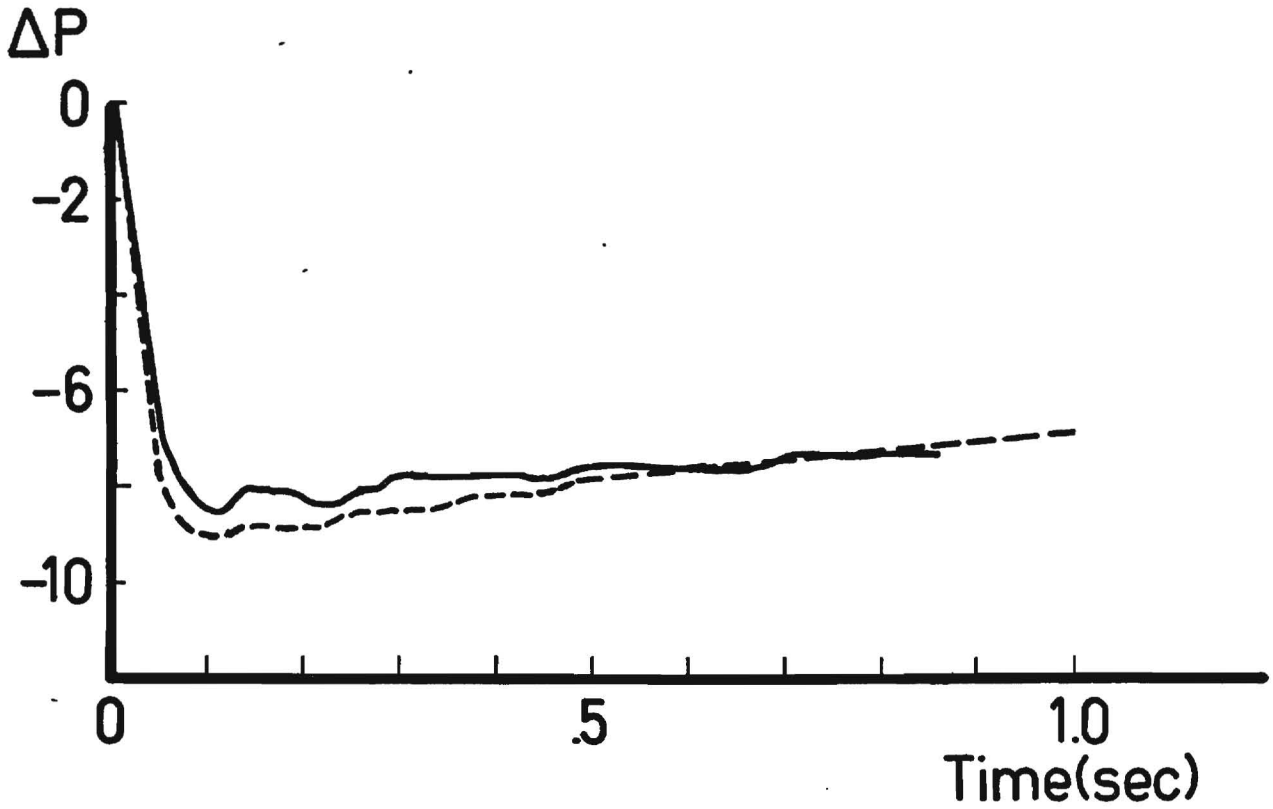
ΔP
0
-2
-6
-10
0
.5
1.0
Time(sec)

Figure 5.5 Slurry results - experimental and simulated pressure curves

ΔP (psi) vs Time (seconds), 20% slurry

Upper: 3-7.7 closing

—— experimental

---- simulation f = .0062

V_i = 5.29 ft/sec

V_f = 3.34 ft/sec

Lower: 7-10 closing

—— experimental

---- simulation f = .0069

V_i = 4.09 ft/sec

V_f = 1.05 ft/sec

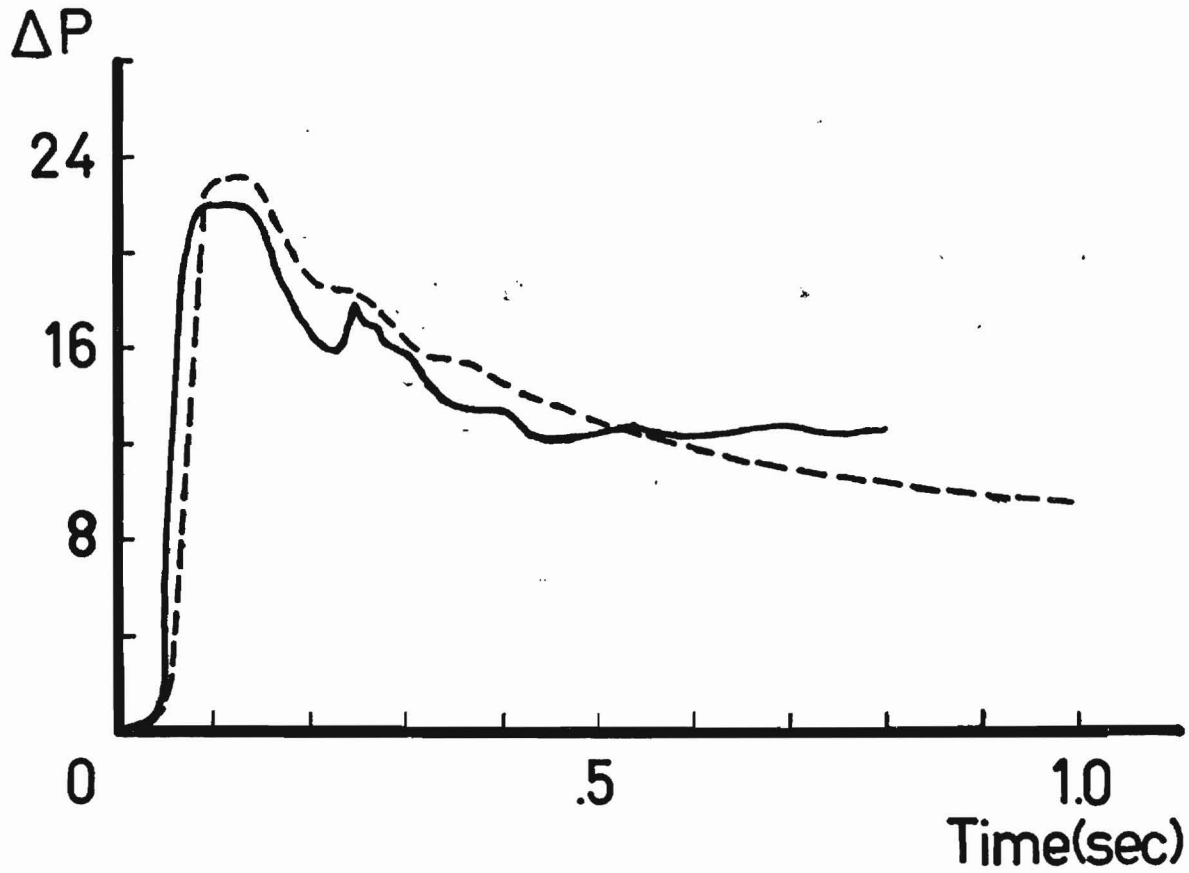
ΔP
24
16
8
0
.5
1.0
Time(sec)

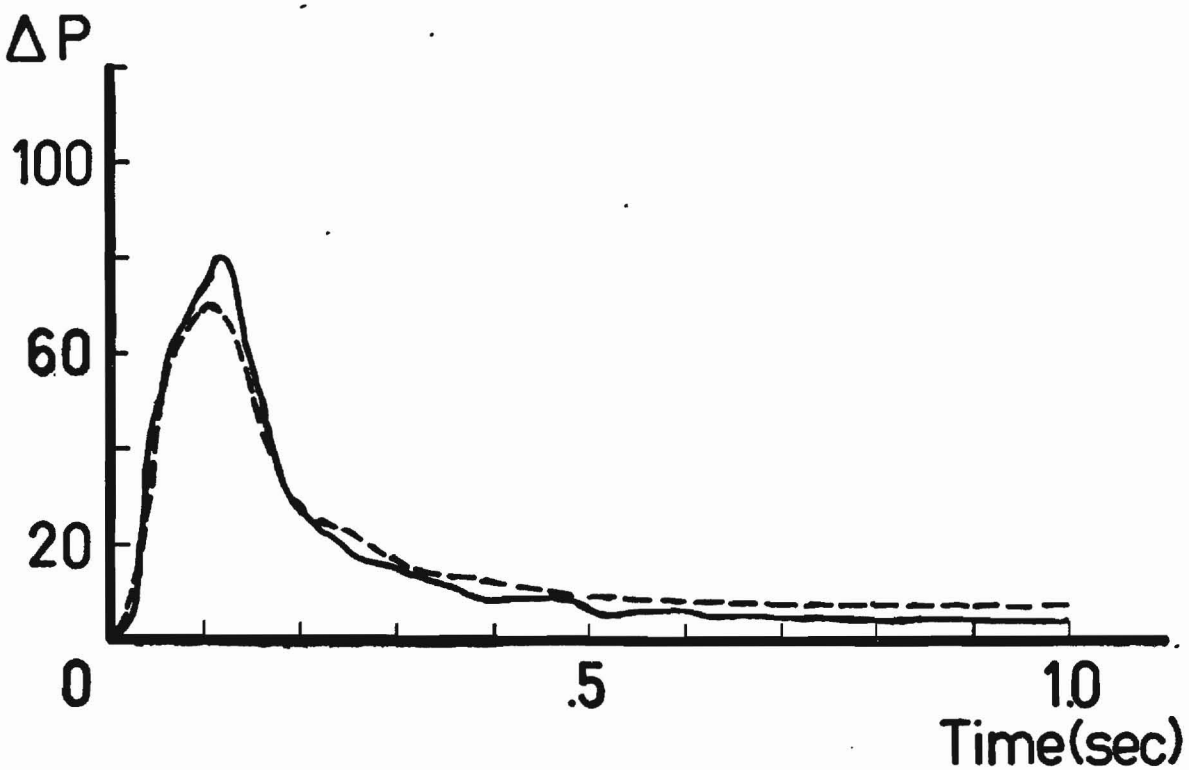
ΔP
100
60
20
0
.5
1.0
Time(sec)

Figure 5.6 Slurry results - experimental and simulated pressure curves

ΔP (psi) vs Time (seconds), 20% slurry

Upper: 3-15 opening

——— experimental

----- simulation f = .0062

V_i = 0.0 ft/sec

V_f = 5.29 ft/sec

Lower: 7-10 opening

——— experimental

----- simulation f = .0065

V_i = 1.97 ft/sec

V_f = 4.43 ft/sec

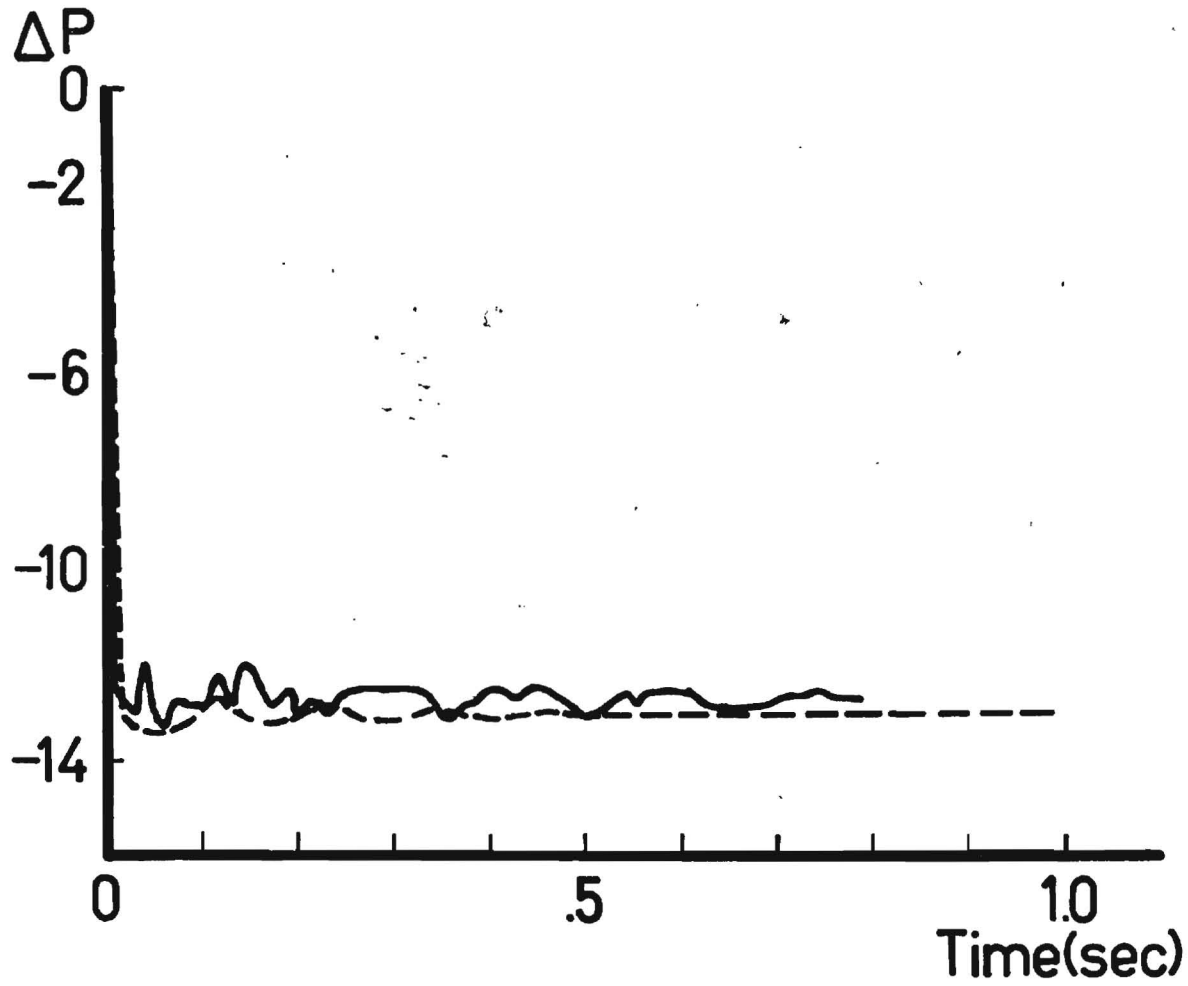
ΔP
0
-2
-6
-10
-14
0
.5
1.0
Time(sec)

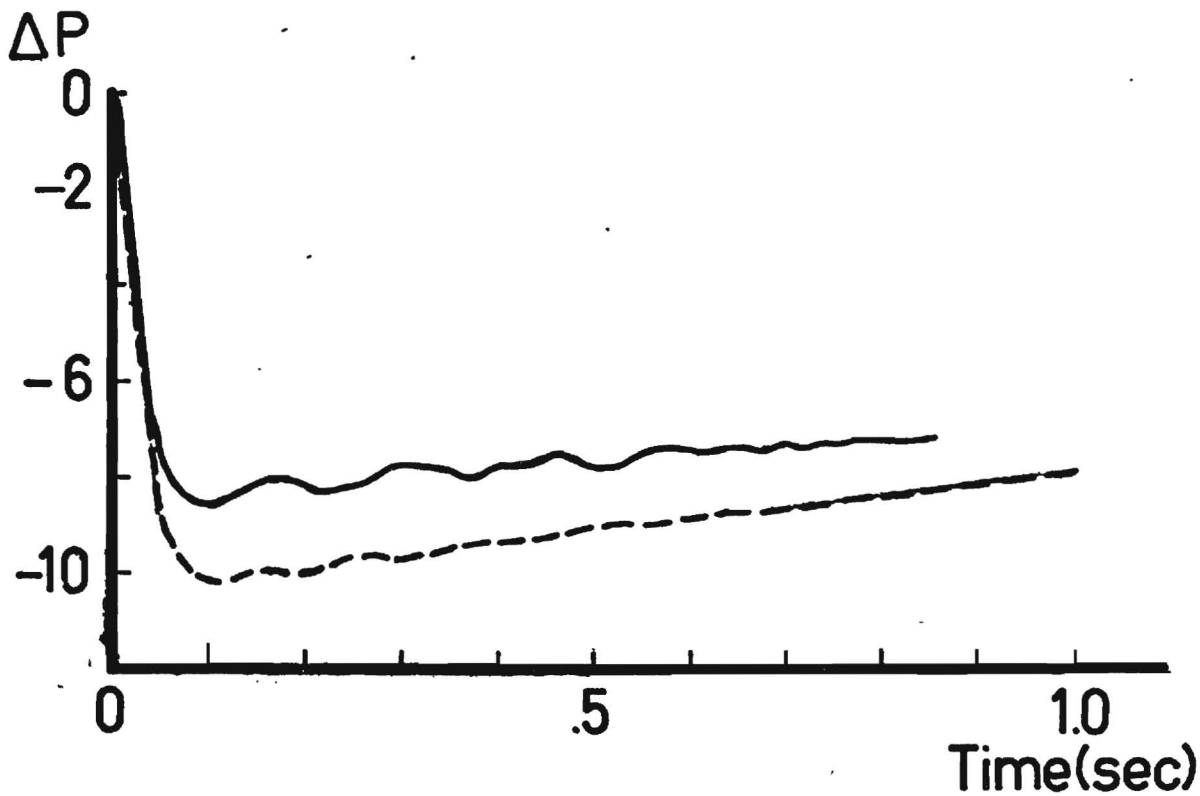
ΔP
0
-2
-6
-10
0
.5
1.0
Time(sec)

Figure 5.7 Slurry results - experimental and simulated pressure curves

ΔP (psi) vs Time (seconds), 30% slurry

Upper: 3-7.7 closing

——— experimental

----- simulation f = .0054

V_i = 5.68 ft/sec

V_f = 3.95 ft/sec

Lower: 7-10 closing

——— experimental

----- simulation f = .0065

V_i = 4.12 ft/sec

V_f = 1.3 ft/sec

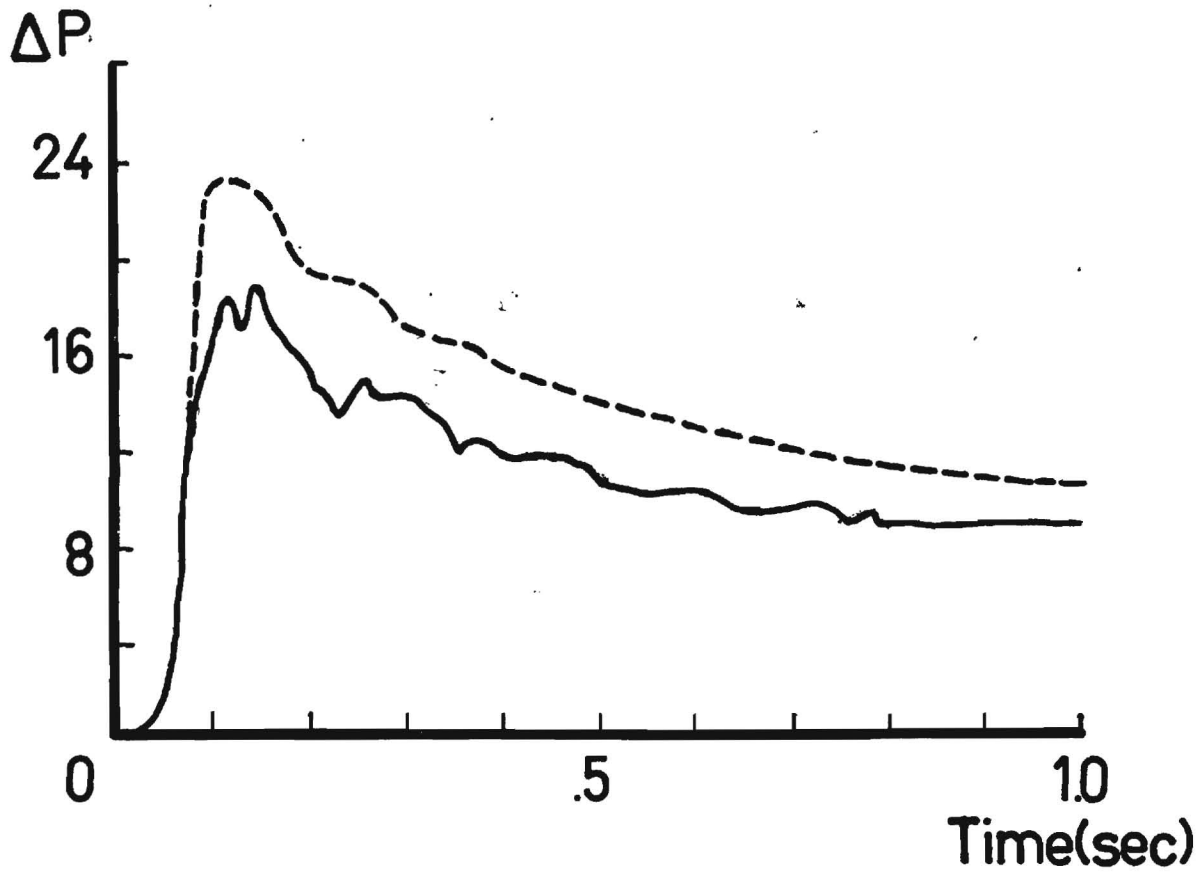
ΔP
24
16
8
0
.5
1.0
Time(sec)

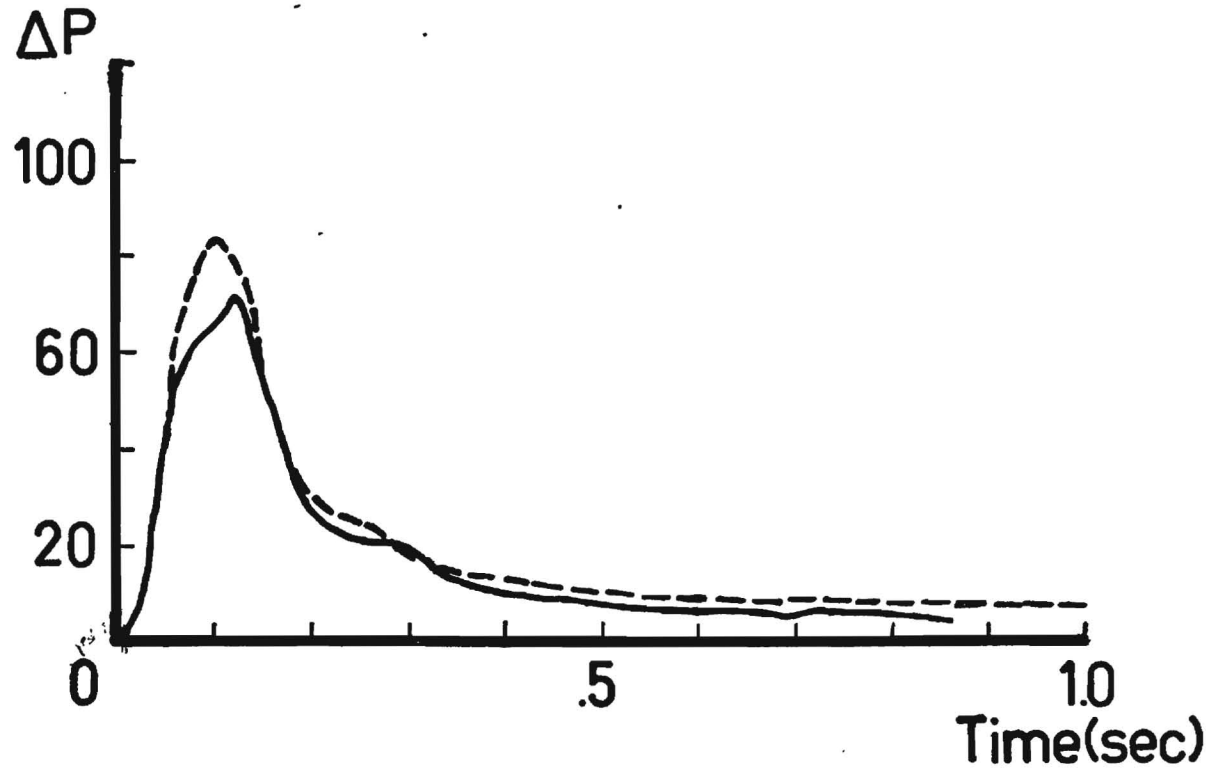
ΔP
100
60
20
0
.5
1.0
Time(sec)

Figure 5.8 Slurry results - experimental and simulated pressure curves
ΔP (psi) vs Time (seconds), 30% slurry

Upper: 3-15 opening

——— experimental

----- simulation f = .0054

V_i = 0.0 ft/sec

V_f = 5.68 ft/sec

Lower: 7-10 opening

——— experimental

----- simulation f = .0047

V_i = 2.32 ft/sec

V_f = 5.0 ft/sec

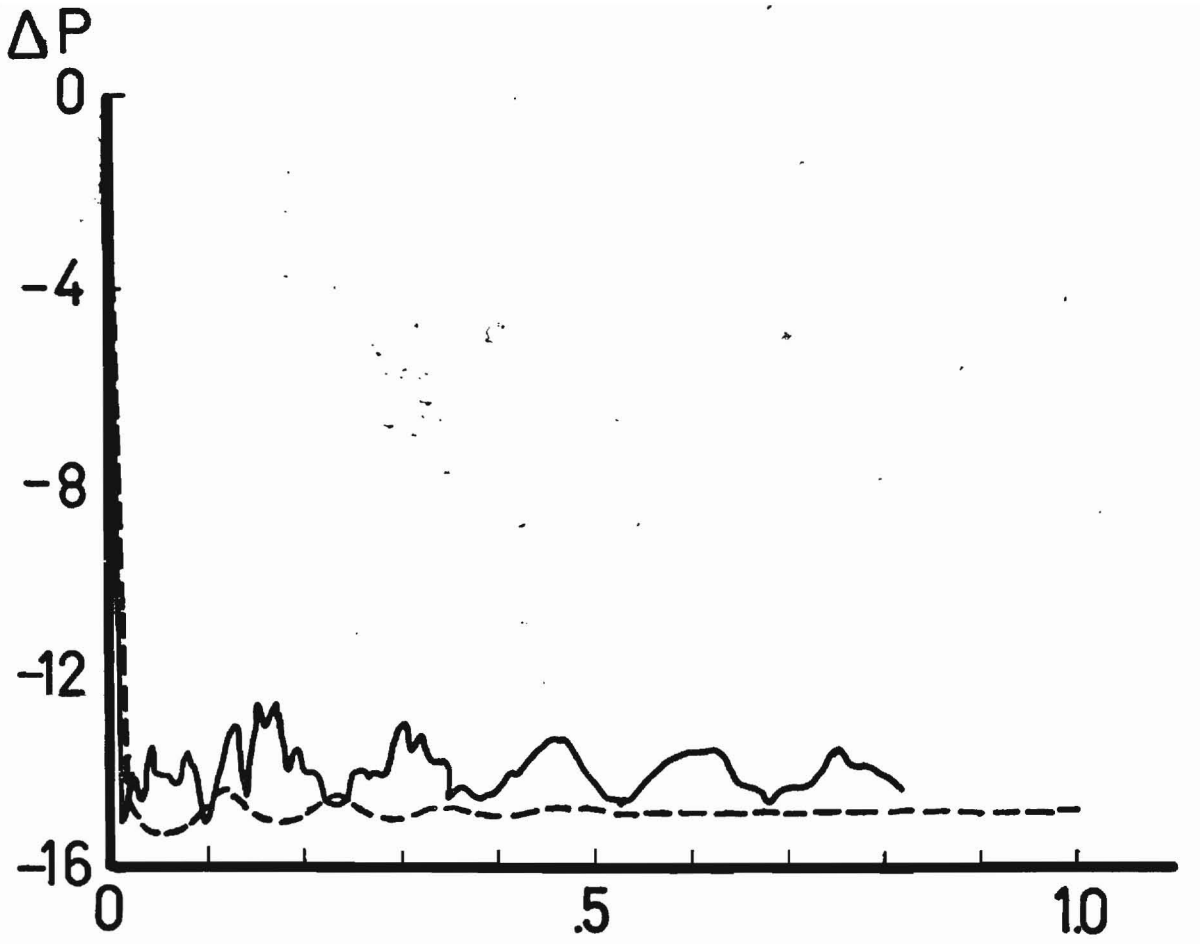
ΔP
0
-4
-8
-12
-16
0
.5
1.0
Time(sec)

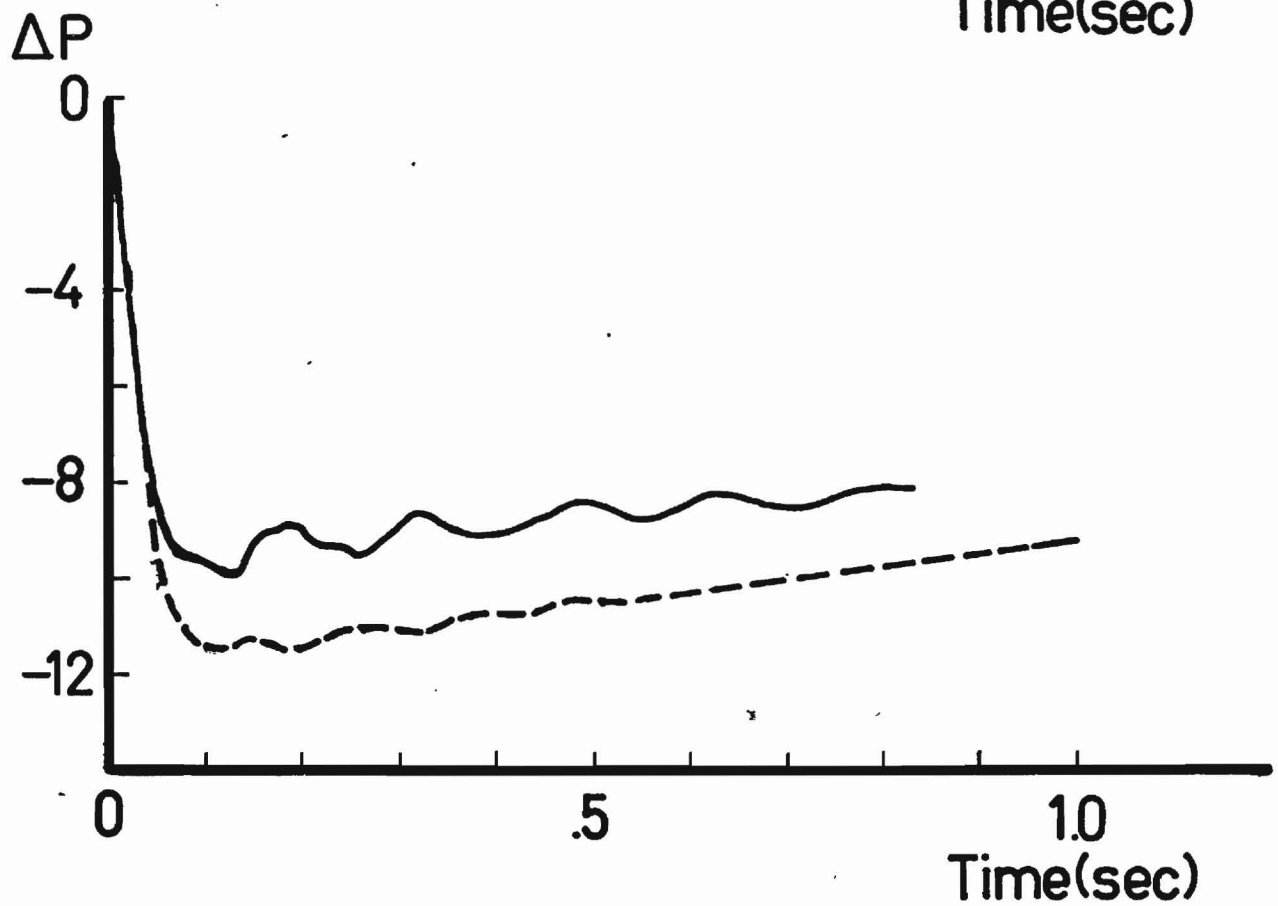
ΔP
0
-4
-8
-12
0
.5
1.0
Time(sec)

Figure 5.9 Slurry results - experimental and simulated pressure curves

ΔP (psi) vs Time (seconds), 35% slurry

Upper: 3-7.7 closing

——— experimental

----- simulation f = .0055

V_i = 5.55 ft/sec

V_f = 3.77 ft/sec

Lower: 7-10 closing

——— experimental

----- simulation f = .0061

V_i = 4.27 ft/sec

V_f = 1.54 ft/sec

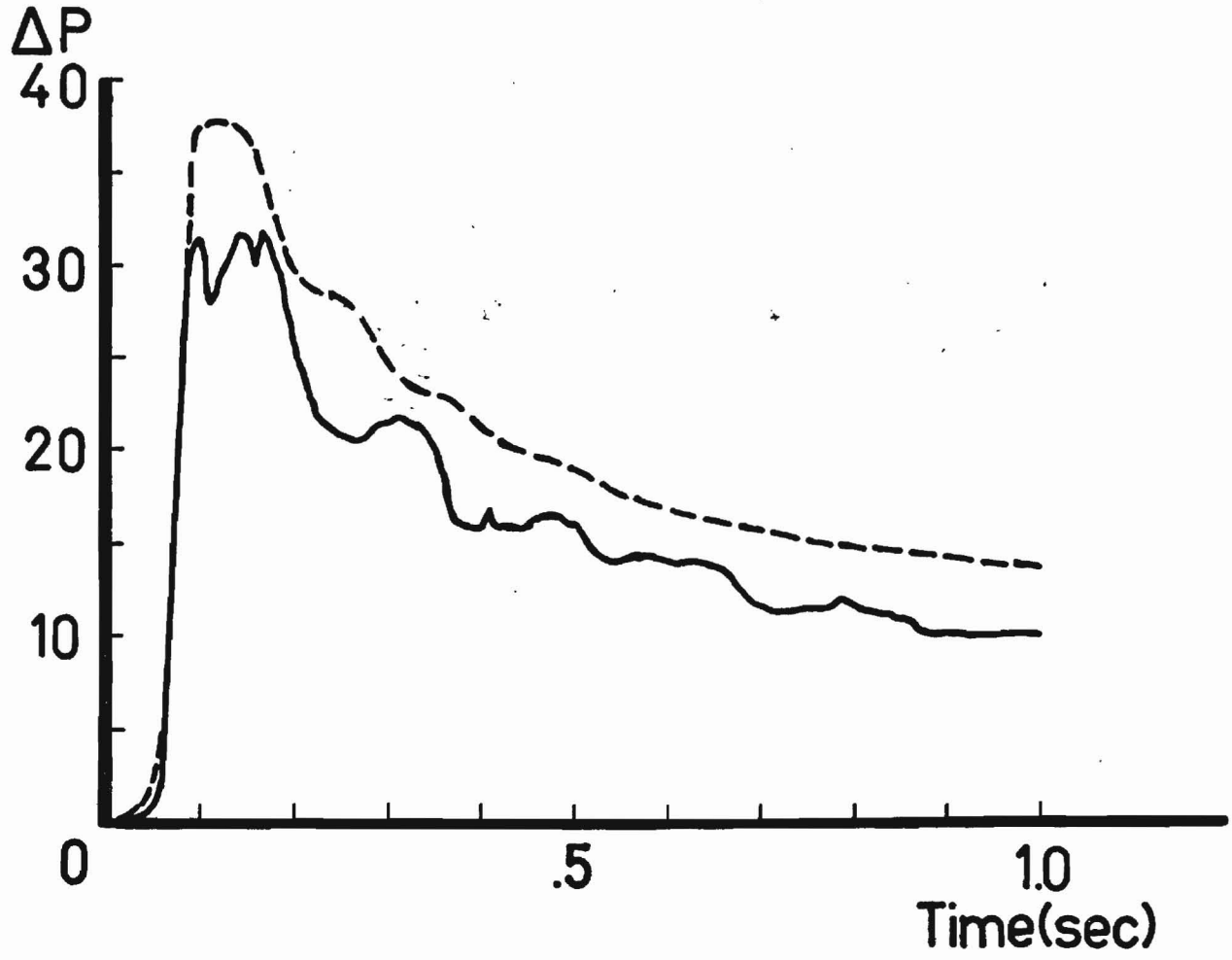
ΔP
40
30
20
10
0
.5
1.0
Time(sec)

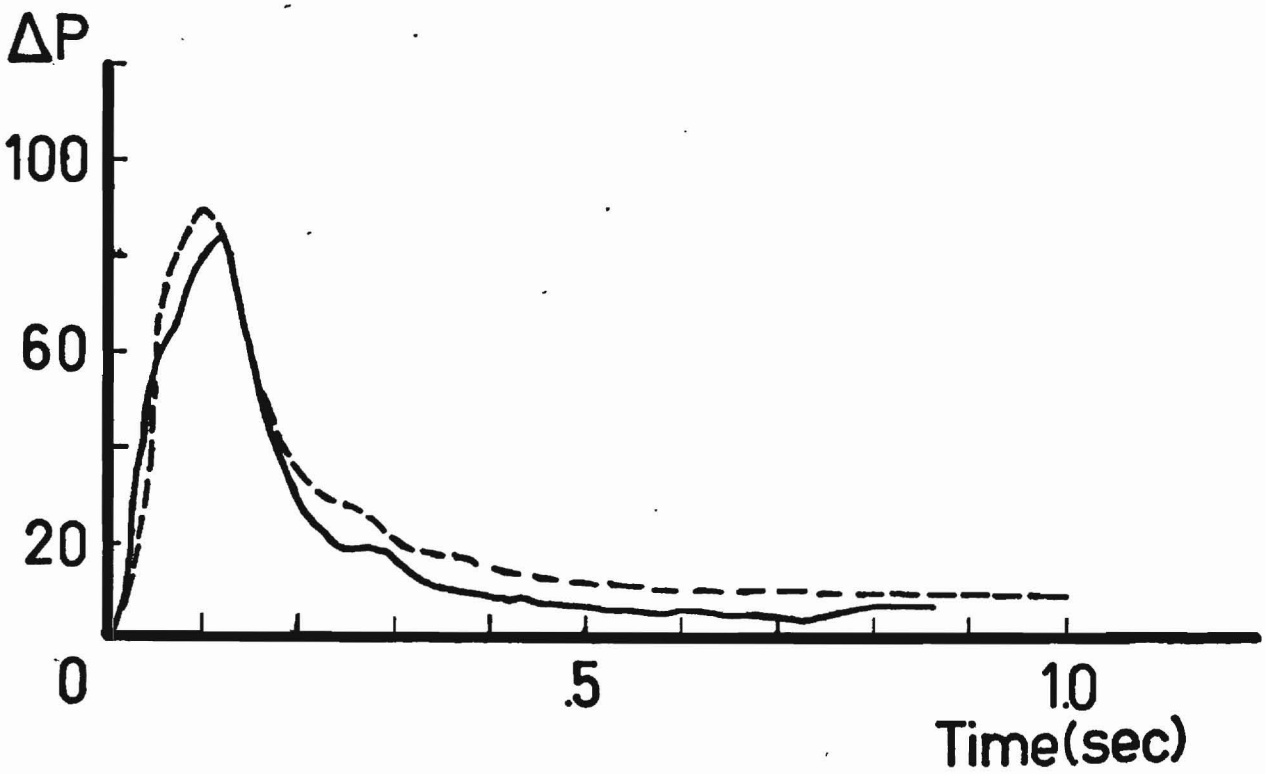
ΔP
100
60
20
0
.5
1.0
Time(sec)

Figure 5.10 Slurry results - experimental and simulated pressure curves

ΔP (psi) vs Time (seconds), 35% slurry

Upper: 3-15 opening

——— experimental

----- simulation f = .0055

V_i = 0.0 ft/sec

V_f = 5.55 ft/sec

Lower: 7-10 opening

——— experimental

----- simulation f = .0047

V_i = 2.33 ft/sec

V_f = 5.05 ft/sec

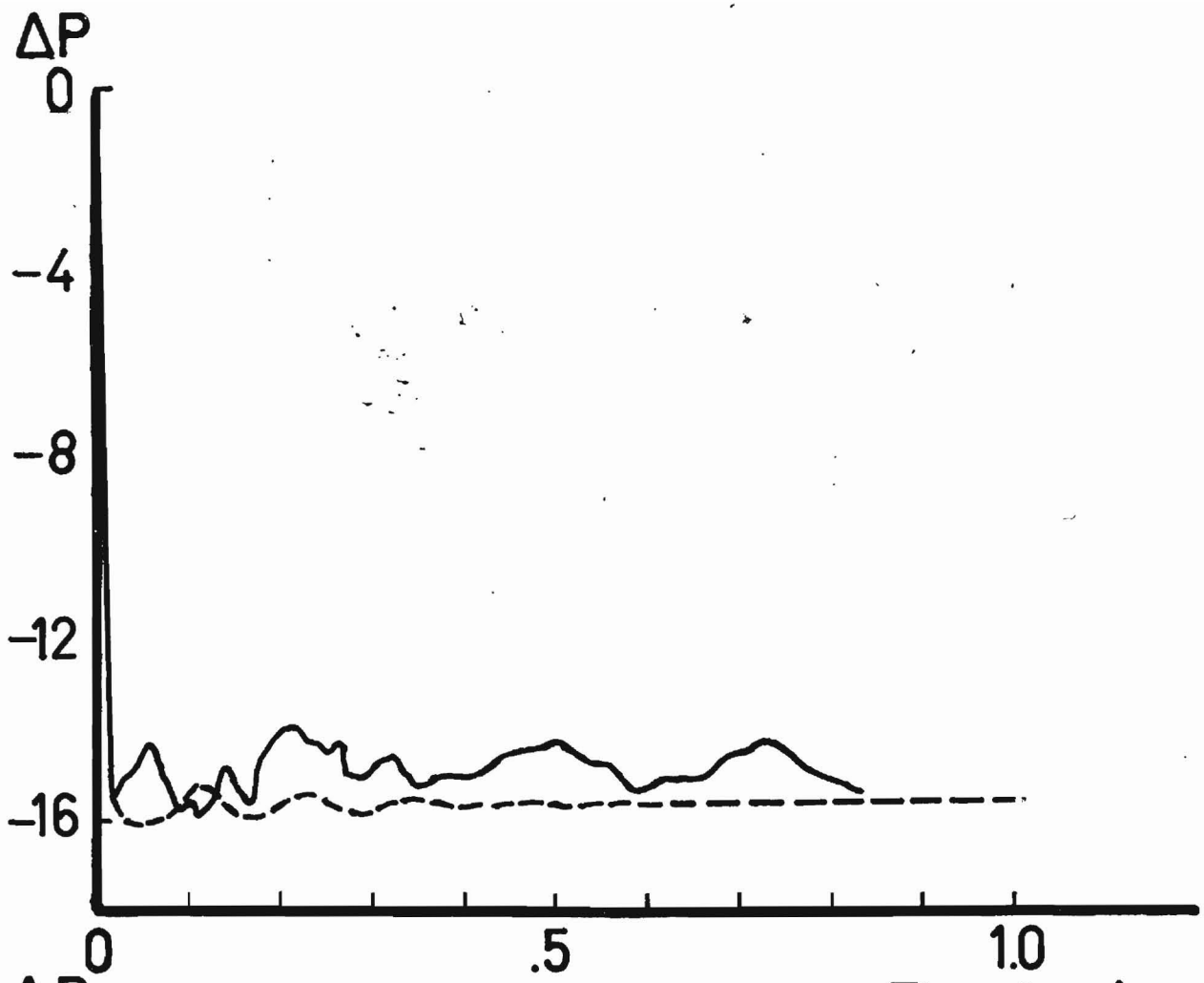
ΔP
0
-4
-8
-12
-16
0
.5
1.0
Time(sec)

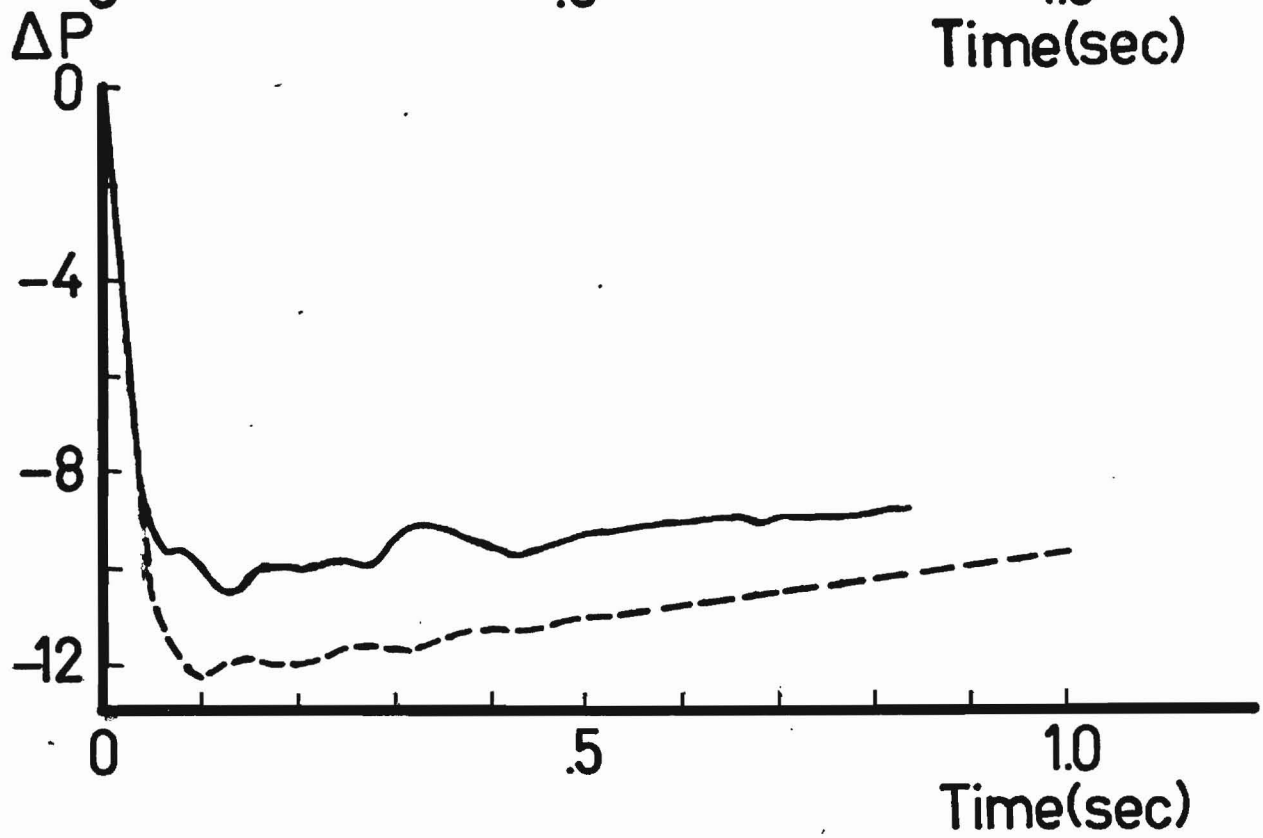
ΔP
0
-4
-8
-12
0
.5
1.0
Time(sec)

position determines the flowrate, a small error in either the initial or final control pressure will cause a flowrate change different from that being simulated, with a resulting difference in the simulated curve from the experimental trace. This problem is not serious in cases in which the initial and/or final valve position is fully open or fully closed since these are well defined positions and are easily set with the signal pressure.

The velocity of sound used for all slurry simulations was 4000 ft/sec. For the particular solids density of the limestone, the calculated velocity of sound is quite independent of the concentration (Reference 2).

5.3 Effect of friction factor on the simulation

Figures 5.11 and 5.12 illustrate the effect of the friction factor upon the simulation for the 35% slurry. For the case of 3-7.7 closing (Figure 5.11 - Upper) the simulation is extremely sensitive to the friction factor used. A friction factor of .0055 was the experimentally determined friction factor. It was obtained by multiplying the friction factor for water (in the corresponding run) by the square of the ratio of the water velocity to slurry velocity. As the amount of stratification within the system becomes less (solids concentration increased) the experimental friction factor approaches that obtained from the friction factor versus Reynolds number and Hedstrom number curve. Using the experimental friction factor maintains the equivalent length of the system constant.

For the case of 7-10 closing (Figure 5.11 - lower) the transient peak pressure is dependent on the friction factor but the final steady

Figure 5.11 Effect of friction factor

ΔP (psi) vs Time (seconds), 35% slurry

Upper: 3-7.7 closing

——— experimental

----- simulations Friction factors in same order as simulation curves.

Lower: 7-10 closing

——— experimental

----- simulations Friction factors in same order as simulation curves.

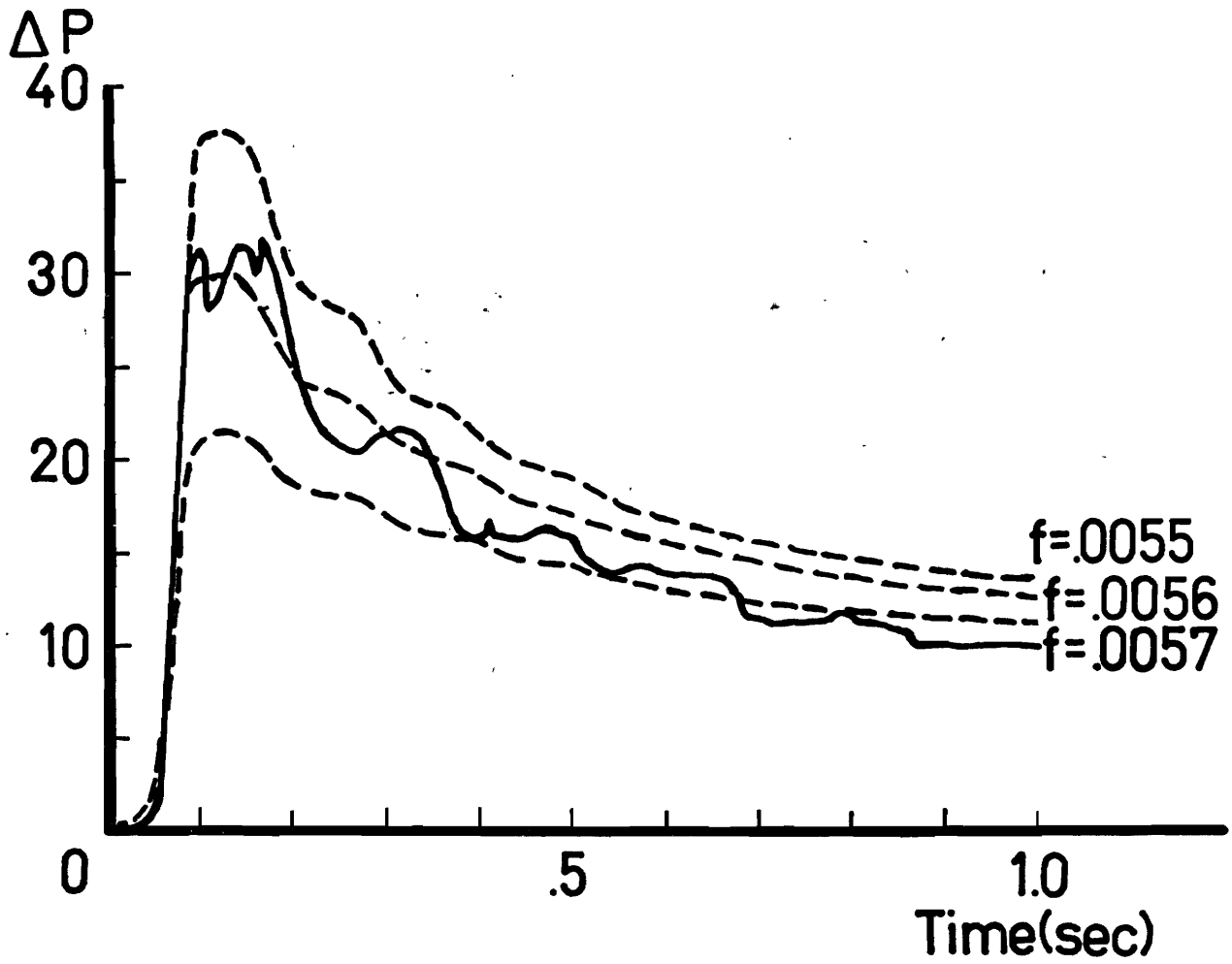
ΔP
40
30
20
10
0
.5
1.0
Time(sec)
f=.0055
f=.0056
f=.0057

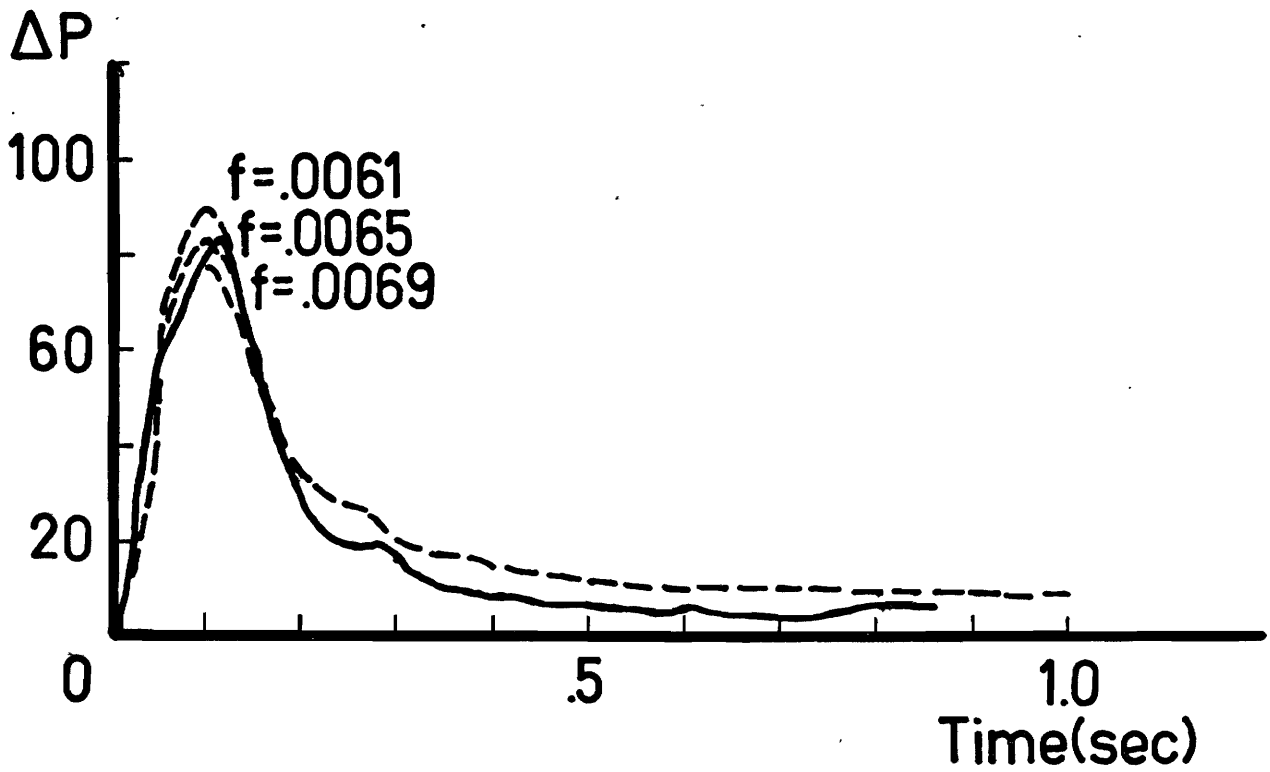
ΔP
100
60
20
0
.5
1.0
Time(sec)
f=.0061
f=.0065
f=.0069

Figure 5.12 Effect of friction factor

ΔP (psi) vs Time (seconds), 35% slurry

Upper: 3-15 opening

——— experimental

----- simulations Friction factors in same order as simulation curves.

Lower: 7-10 opening

——— experimental

----- simulations Friction factors in same order as simulation curves.

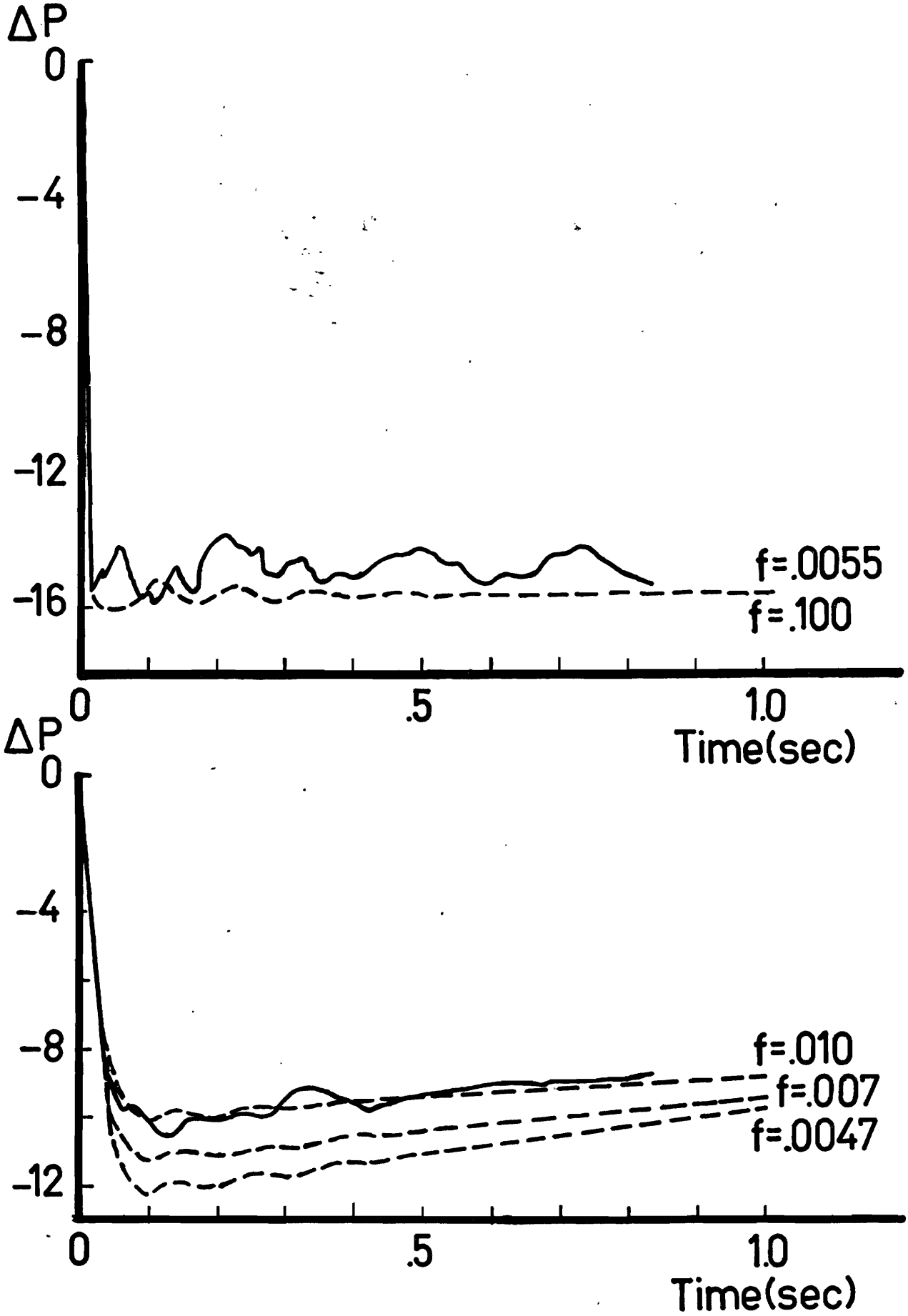
ΔP
0
-4
-8
-12
-16
f=.0055
f=.100
0
.5
1.0
Time(sec)
ΔP
0
-4
-8
-12
f=.010
f=.007
f=.0047
0
.5
1.0
Time(sec)

state is not. The experimental friction factor is .0061.

For the case of 3-15 opening (Figure 5.12 - Upper) the simulation is independent of the friction factor in as far as the pressure change is concerned. However the final steady state velocity is quite dependent on the friction factor. The experimental friction factor is 0.0055, and this gives a final steady state velocity approaching that which is experimentally observed. A much higher friction factor has the effect of reducing this velocity but not changing the pressure wave simulation. Since there is no flow initially in this case, one would expect the friction factor to decrease continuously from an infinite value at no flow. This large change in the friction factor in the experimental situation implies that the simulation is not adequate in this case and that lack of agreement with the experimental data should not be surprising.

For the case of 7-10 opening (Figure 5.12 - Lower), the simulation is again moderately dependent on the friction factor. The experimental friction factor is .0047. Again, it is necessary to use this friction factor to obtain reasonable steady state velocity simulations. As stated earlier, the offset in the simulation from the experimental curve is the result of experimental error in the settings of the control pressures for the valve.

In general the simulations based on the experimental friction factors are close to the experimental curves. The experimental friction factor should be used instead of the theoretical friction factors where any degree of stratification is possible, since the experimental ones range from 0-100% higher than the theoretical values depending on the degree of stratification.

5.4 Startup results - Settled slurries

The results of experimental startups on settled 20% and 35% slurries are shown in Figures 5.13 and 5.14. A settled slurry refers to the situation in which the pipeline has been shutdown with the horizontal section full of slurry for a period of time long enough to allow the solids to settle. Startup tests were made on 20%, 30%, and 35% slurries at various time intervals and all curves were characteristically the same as the two shown.

The following general observations could be made about all startup curves.

A low frequency, high amplitude oscillation resembling the behavior of an underdamped second order system was observed in all cases. The highest amplitudes were observed for 20% slurries (no reliable data was obtained at 10%), and damping appeared to increase with slurry concentration.

The period of the fluctuation was approximately 0.2 seconds for all concentrations. All other curves, except for the startup of an unsettled 35% slurry, had a period of approximately 0.1 to 0.15 seconds. The explanation for this increase in the period of the wave is a decrease in the speed of sound. This reduction could arise from the fact that the solid bed is probably much more compressible than the pipe. This elasticity of the boundaries could cause a significant reduction in the velocity of sound.

The time required to reach maximum pressure drop was in all cases approximately 0.1 seconds. This was true for all concentrations if sufficient time for complete settling was allowed. In contrast the

Figure 5.13 Experimental startup pressure curve - 20% slurry

ΔP (psi) vs Time (seconds)

18 hours of settling before startup

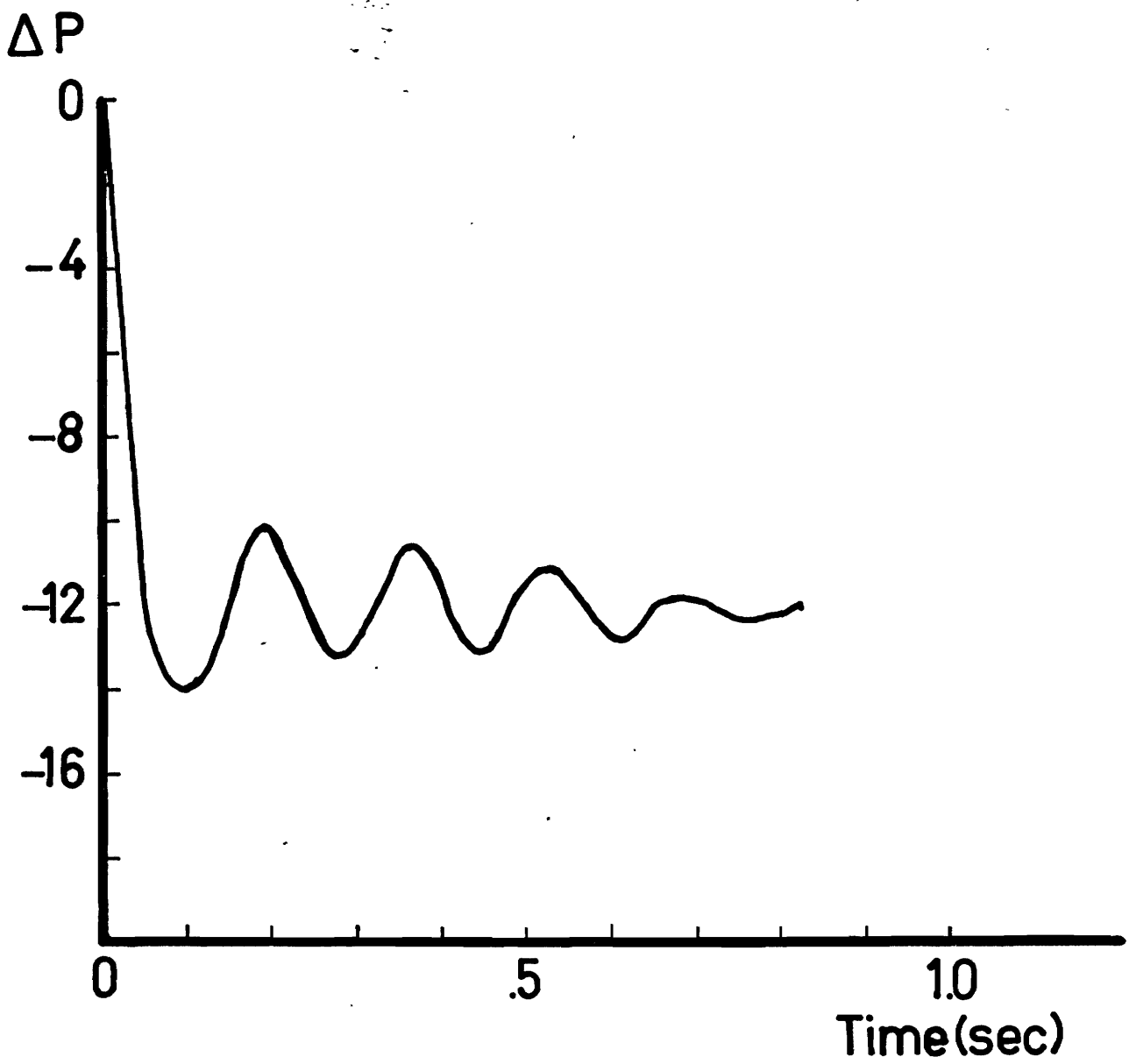
ΔP
0
-4
-8
-12
-16
0
.5
1.0
Time(sec)

Figure 5.14 Experimental startup pressure curve - 35% slurry

ΔP (psi) vs Time (seconds)

4 hours of settling before startup

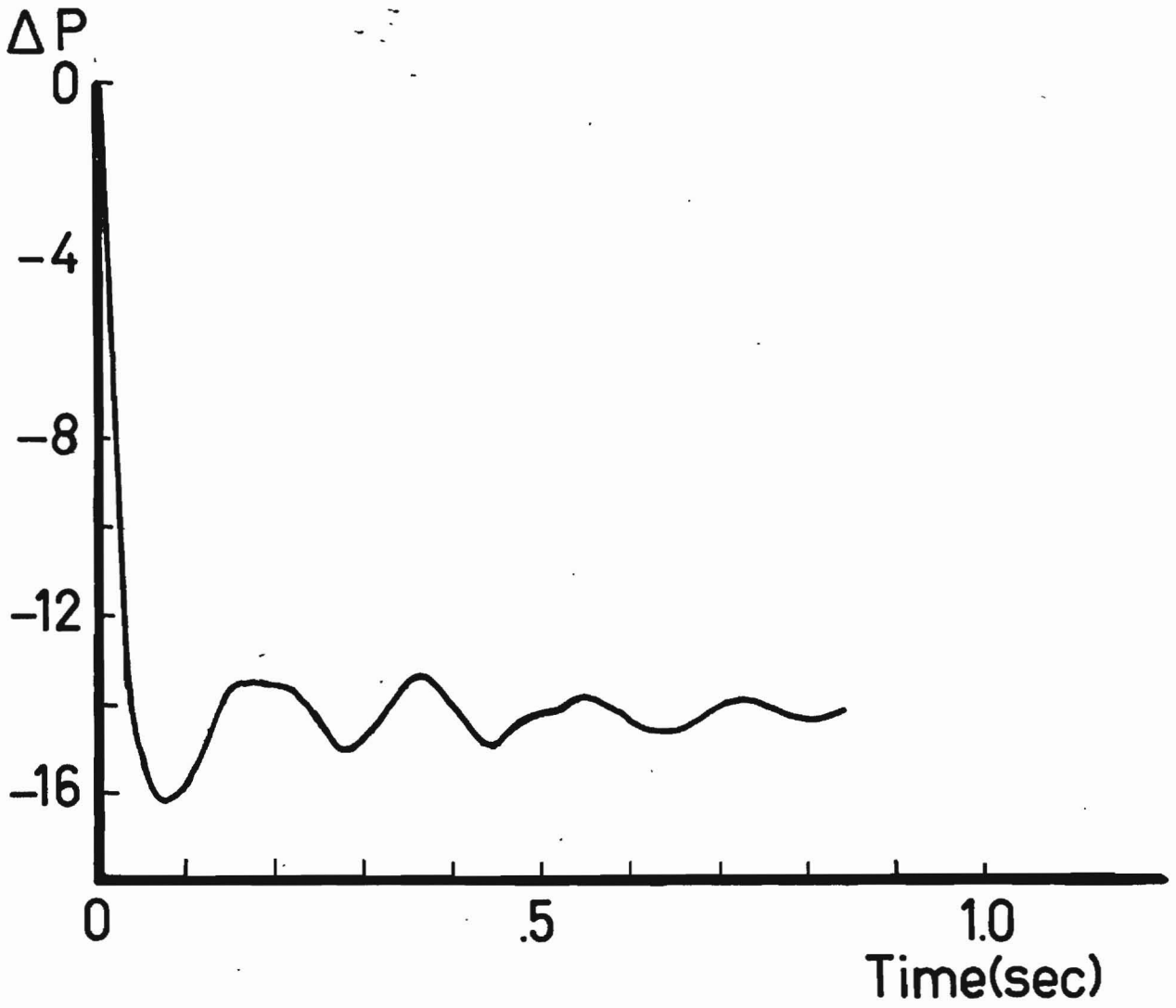
ΔP
0
-4
-8
-12
-16
0
.5
1.0
Time(sec)

pressure wave in startups of unsettled slurry reached a minimum almost instantaneously. One experiment was conducted after 18 days of settling and the time for maximum pressure change in this case was 0.13 seconds. These results indicate that the solid bed hinders the start of flow to a small extent.

Analysis of the cine´ films indicated the establishment of flow above the settled bed almost immediately upon opening of the valve. The bed did not move but was gradually eroded away. The time required for erosion to begin was somewhat dependent on the length of time the bed had settled, ranging from 0.29 seconds for a 6 hour settling period to 0.92 seconds for a 2 week settling period (35% slurry). It was impossible to visually detect any phenomena within the pipeline after 1-1½ seconds since the solids were well dispersed in the line by this time. Indications are however that the pressure wave was damped out well before the solid bed was completely eroded away.

There is also some evidence that erosion may not begin at all points within the pipeline at the same time. Frame-by-frame analysis of the film for 6 hours settling showed ripples forming along the solid bed at the start of erosion. The two week startup showed a wave of suspended solids entering the sightglass region from upstream, indicating prior erosion of the bed upstream. The time at which this wave appeared was 0.92 seconds, long before a continuity wave from the head tank could arrive. Erosion of the bed in the sightglass region began concurrently with the arrival of the wave of suspended solids.

CHAPTER 6. CONCLUSIONS AND RECOMMENDATIONS FOR FURTHER WORK

6.1 Conclusions

1. The computer program based on a constant steady state friction factor and slurry bulk properties provides a reasonable simulation of the transient pressure wave during flow changes for a homogeneous slurry mixture. The friction factor must be altered from the theoretical value if stratification is significant.

2. The simulation is not very good for a system in which a solid bed has formed.

3. The unsettled limestone slurry exhibits no significant startup problems up to concentrations of 35% by volume.

4. Settled limestone slurries, up to 35% by volume, in horizontal systems exhibit no major startup difficulties. Settling in vertical or inclined lines, in which the pipe may become completely sealed with solids, can be expected to present major startup difficulties due to a very high yield stress of the solids.

6.2 Suggestions for further work

1. The computer program could be modified to make the friction factor a function of the velocity and position within the pipeline.

2. Experimental measurements of the pressure waves in other slurry systems could be made. Of special interest would be a slurry exhibiting significant stratification during flow at velocities similar to those used in this study. At high degrees of stratification the effect on the

pressure wave may be similiar to that during startup of a stationary bed.

3. A small cable could be attached to the valve stem of the control valve. This cable, if connected through a spring to a load transducer, could provide an accurate indication of the valve rotation for each trial. The signal from the load transducer could be recorded on a calibrated strip recorder. This would eliminate some of the difficulty associated with positioning the valve with the signal pressure.

LIST OF REFERENCES

1. Streeter, V.L., Waterhammer Analysis with Nonlinear Frictional Resistance, "Hydraulics and Fluid Mechanics", ed.,Richard Silvester, The Macmillan Company, 1964.

2. Wood, D.J. and Kao, T.Y.,"Unsteady Flow of Solid-Liquid Suspensions", A.S.C.E. - Proc. v92 (J. Eng. Mechanics Div.),p117 - 134, 1966.

3. Streeter, V.L., "Handbook of Fluid Mechanics", 1st edition, McGraw-Hill Book Company, Inc.,1961.

4. Parmakian, J., "Waterhammer Analysis", Prentice-Hall, Inc.,1955.

5. National Research Council of The United States of America, "International Critical Tables", Vol.2, McGraw-Hill, p51, 1927.

APPENDIX A.

Computer simulation program:

The computer program used for the simulation of the pressure wave is written in Fortran IV with WatFIV. The valve characeristics shown in the program (lines 67-73) are for the case of control pressures 7-10 opening. The valve characteristics for the three other flow changes studied are also shown. The data input must be provided as described in Format 1 in the program. The data input includes the following:

D - pipe diameter (feet)

F - friction factor

VSS - initial steady state velocity (feet/second)

N - number of characteristic points along pipeline

G - acceleration of gravity (feet/second^2)

A - velocity of sound in the system (feet/second)

TFVM - time at which valve motion stops (seconds)

Z3 - elevation of valve above datum (feet), 0 feet for this system

Z0 - elevation of head tank outlet above datum (feet), 23.46 feet for this system

RO - density of slurry (lb_m/ft^3)

CV0 - CV value for the initial valve setting except for the case in which the initial flow is zero. In this case CV0 is CV for the final valve position.

There are two statements which must be provided for the special case of valve opening from closed to fully open (control pressure 3-15 psig).

These are statements numbered 24 and 11 (lines 38 and 40 respectively). DELPO is normally the pressure drop across the valve at the initial steady state flowrate. Since there is no initial flow, DELPO in statement 24 is redefined as the pressure drop across the valve at the final flowrate. This can be calculated from the valve flow equation:

$$\Delta P = (Q/CV)^2 G \quad \ldots\ldots\ldots\ldots\ldots\ldots\ldots\ldots\ldots\ldots \quad (A.1)$$

where ΔP is the pressure drop across the valve (psi)

Q is the flow in GPM (Imperial)

CV is the valve constant in GPM (Imperial)

G is the specific gravity

DELPO is in units of pounds/square foot in the program, hence the multiplier of 144.

Statement 11 provides VSS as the final steady state velocity, however VSS must be inserted in the data card as 0., the initial steady state velocity. Statements 24 and 11 have no effect on the program unless VSS is 0. on the data card.

```
$JOB WATFIV    168400,L.T.HUBBARD,TIME=30
      IMPLICIT  REAL(L)
      INTEGER U,W
      DIMENSION V(20),VP(20),PT(20),PP(20)
      READ(5,1)D,F,VSS,N,S,A,TFVM,Z3,Z0,RO,CVO
    1 FORMAT(3F5.0,I2,7F5.0)
      GC=32.2
C STEADY  STATE  RELATIONSHIP
      LT=229.
      IF(VSS.EQ.0.)GO TO 23
      LO=(-((VSS**2)*D/2.)+G*(Z0-Z3)*D)/(2*F*(VSS**2))
   23 FC=F*1.51
      T=0.
      U=0
      TAU=1.
      DELT=LT/(N*A*2)
      DELTX=LT/N
      TRANDS=5.0
      XPC=2.42
      XGR=8.38
C  CALCULATE  PRESSURE  AT  POINTS  ALONG  LINE
      K=N+1
      KK=N+2
      KKK=N+3
      DO 2 I=1,K
      L=DELTX*(I-1)
      IF(I.EQ.1)Z1=20.46
      IF(I.GT.1.AND.I.LT.11)Z1=2.63
      IF(I.EQ.11)Z1=0.21
      IF(VSS.EQ.0.)GO TO 21
      P=RO*G/GC*(Z0-Z1)-RO*G/GC*(Z0-Z3)*((D+4*FC*L)/(D+4*F*LO))
      GO TO 22
   21 P=RO*G/GC*(Z0-Z1)
   22 V(I)=VSS
      PP(I)=P/144.
    2 PT(I)=P
      PO=PT(11)
      IF(VSS.EQ.0.) GO TO 24
      DELPO=PO
      GO TO 25
   24 DELPO=0.433*144.
      TAU=0.
   11 VSS=5.55
C V(12) ANDPP(12) REFER TO VELOCITY AND PRESSURE AT TRANSDUCER
   25 V(12)=V(11)-TRANDS/DELTX*(V(11)-V(10))
      PT(12)=PT(11)-TRANDS/DELTX*(PT(11)-PT(10))-2.42*RO*
     1(1-TRANDS/DELTX)
      PP(13)=0.0
      PP(12)=PT(12)/144.
      PTNOT=PP(12)
      WRITE(6,3)
    3 FORMAT('1    VELOCITIES  AND  PRESS  AT  TENTH  POINTS  AND TRANSD
     1UCER  FOR  EQUAL  TIME  INCREMENTS',///,'   TIME     TAU     X/L=
     2    0       .1       .2       .3       .4       .5       .6       .7
     3.8       .9      1.0     TRANS     DELTP')
   20 WRITE(6,4)T,TAU,(V(I),I=1,KK),(PP(I),I=1,KKK)
    4 FORMAT(1H0,2F8.3,4X,3HV= ,12F8.3/1H ,20X,3HP= ,13F8.3)
   30 T=T+DELT
      U=U+1
C  CALCULATION OF INTERIOR  POINTS
      DO 80 J=2,N
      VR=V(J)+DELT/DELTX*A*(V(J-1)-V(J))
```

```
      VS=V(J)+DELT/DELTX*A*(V(J+1)-V(J))
      PR=PT(J)+DELT/DELTX*A*(PT(J-1)-PT(J))
      PS=PT(J)+DELT/DELTX*A*(PT(J+1)-PT(J))
      IF(J.EQ.2) GO TO 12
      PP(J)=A*RO*(VR-VS)/(GC*2.)+(PR+PS)/2.
      VP(J)=(VR+VS)/2.+10.1*(PR-PS)/(A*RO)-FC*2.*V(J)*ABS(V(J))*DELT/D
C     CALCULATION AT POINT 2
      IF(J.NE.2) GO TO 30
   12 PP(2)=(PR+PS)/2.+(A*RO*(VR-VS))/(2.*GC)+XCR*RO*G/(2.*GC)
      VP(2)=(VS+VR)/2.+(GC*(PR-PS))/(A*RO*2.)+G*XCR/(2.*A)-2.*FC*V(2)
     1*ABS(V(2))*DELT/D
   30 CONTINUE
C     BOUNDARY CONDITIONS AT THE RESERVOIR
      VS= V(1)+DELT/DELTX*A*(V(2)-V(1))
      PS=PT(1)+DELT/DELTX*A*(PT(2)-PT(1))
      VP(1)=VS+GC/(A*RO)*(PT(1)-PS)+G*DELT-2.*FC*VS*ABS(VS)*DELT/D
C     BOUNDARY  CONDITIONS  AT  THE  VALVE
      IF(T.GT..1129) GO TO 16
      IF(T.GT.0..AND.T.LE..0161) CV=7.8+76.5*T
      IF(T.GT..0161.AND.T.LE..0323) CV=6.4+177.8*T
      IF(T.GT..0323.AND.T.LE..0484)CV=2.0+310.5*T
      IF(T.GT..0484.AND.T.LE..0645) CV=6.0+230.*T
      IF(T.GT..0645.AND.T.LE..1129) CV=12.+140.*T
   16 IF(T.GT..1129) CV=27.8
      TAU=CV/CVO
      PR=PT(11)+DELT/DELTX*A*(PT(10)-PT(11))
      VR=V(11)+DELT/DELTX*A*(V(10)-V(11))
      C1=GC*DELPO/(A*RO*(VSS**2)*(TAU**2))
      C2=VR+GC*PR/(A*RO)+G*XPC/A-2.*FC*VR*ABS(VR)*DELT/D
      VP(11)=(-1.+SQRT(1.+4.*C1*C2))/(2.*C1)
      PP(11)=(VP(11)/(VSS*TAU))**2*DELPO
C     CONDITIONS  AT  THE  TRANSDUCER
      VP(12)=VP(11)-TRANDS/DELTX*(VP(11)-VP(10))
      PP(12)=PP(11)-TRANDS/DELTX*(PP(11)-PP(10))-2.42*RO*
     1(1-TRANDS/DELTX)
      DO 15 J=1,KK
   15 V(J)=VP(J)
      DO 40 J=2,KK
      PT(J)=PP(J)
   40 PP(J)=PP(J)/144.
      PP(13)=PP(12)-PINOI
C     PRINTOUT  CONTROL
      IF(U.GT.500)  GO TO 10
      IF(U/5*5.EQ.U) GO TO 20
      GO TO 30
   10 STOP
      END

$ENTRY
```

VALVE CHARACTERISTICS (7-10 OPENING)

```
      VS=V(J)+DELT/DELTX*A*(V(J+1)-V(J))
      PR=PT(J)+DELT/DELTX*A*(PT(J-1)-PT(J))
      PS=PT(J)+DELT/DELTX*A*(PT(J+1)-PT(J))
      IF(J.EQ.2) GO TO 12
      PP(J)=A*RO/GC*(VR-VS)/2.+(PR+PS)/2.
      VP(J)=(VR+VS)/2.+16.1*(PR-PS)/(A*RO)-FC*2.*V(J)*ABS(V(J))*DELT/D
C  CALCULATION AT POINT 2
      IF(J.NE.2) GO TO 80
   12 PP(2)=(PR+PS)/2.+A*RO/GC*(VR-VS)/2.+XCR*RO*G/(2.*GC)
      VP(2)=(VS+VR)/2.+GC/(A*RO)*(PR-PS)/2.+G*XCR/(2.*A)-2.*FC*V(2)
     1*ABS(V(2))*DELT/D
   80 CONTINUE
C  BOUNDARY CONDITIONS AT THE RESERVOIR
      VS= V(1)+DELT/DELTX*A*(V(2)-V(1))
      PS=PT(1)+DELT/DELTX*A*(PT(2)-PT(1))
      VP(1)=VS+GC/(A*RO)*(PT(1)-PS)+G*DELT-2.*FC*VS*ABS(VS)*DELT/D
C  BOUNDARY  CONDITIONS  AT  THE  VALVE
      IF(T.GT..1934) GO TO 16
      IF(T.GT.0..AND.T.LE..0161)CV=0.+217.*T
      IF(T.GT..0161.AND.T.LE..0323)CV=-2.5+387.*T
      IF(T.GT..0323.AND.T.LE..0484)CV=3.5+196.5*T
      IF(T.GT..0484.AND.T.LE..0645)CV=-1.5+303.*T
      IF(T.GT..0645.AND.T.LE..0968)CV=-11.5+460.*T
      IF(T.GT..0968.AND.T.LE..1129)CV=-31.+665.*T
      IF(T.GT..1129.AND.T.LE..1290)CV=-77.5+1081.*T
      IF(T.GT..1290.AND.T.LE..1371)CV=-110.+1341.*T
      IF(T.GT..1371.AND.T.LE..1451)CV=-13.5+637.*T
      IF(T.GT..1451.AND.T.LE..1532)CV=31.+331.*T
      IF(T.GT..1532.AND.T.LE..1612)CV=49.5+211.*T
      IF(T.GT..1612.AND.T.LE..1693)CV=30.25+332.*T
      IF(T.GT..1693.AND.T.LE..1773)CV=0.+513.*T
      IF(T.GT..1773.AND.T.LE..1854)CV=40.5+285.5*T
      IF(T.GT..1854.AND.T.LE..1934)CV=78.5+80.1*T
   16 IF(T.GT..1934)CV=94.
      TAU=CV/CVO
      PR=PT(11)+DELT/DELTX*A*(PT(10)-PT(11))
      VR=V(11)+DELT/DELTX*A*(V(10)-V(11))
      C1=GC*DELPO/(A*RO*(VSS**2)*(TAU**2))
      C2=VR+GC*PR/(A*RO)+G*XPC/A-2.*FC*VR*ABS(VR)*DELT/D
      VP(11)=(-1.+SQRT(1.+4.*C1*C2))/(2.*C1)
      PP(11)=(VP(11)/(VSS*TAU))**2*DELPO
C  CONDITIONS  AT  THE  TRANSDUCER
      VP(12)=VP(11)-TRANDS/DELTX*(VP(11)-VP(10))
      PP(12)=PP(11)-TRANDS/DELTX*(PP(11)-PP(10))-2.42*RO*
     1(1-TRANDS/DELTX)
      DO 15 J=1,KK
   15 V(J)=VP(J)
      DO 40 J=2,KK
      PT(J)=PP(J)
   40 PP(J)=PP(J)/144.
      PP(13)=PP(12)-PTNOT
C  PRINTOUT  CONTROL
      IF(U.GT.500)  GO TO 10
      IF(U/5*5.EQ.U) GO TO 20
      GO TO 30
   10 STOP
      END

$ENTRY
```

VALVE CHARACTERISTICS (3-15 OPENING)

```
      PR=PT(J)+DELT/DELTX*A*(PT(J-1)-PT(J))
      PS=PT(J)+DELT/DELTX*A*(PT(J+1)-PT(J))
      IF(J.EQ.2) GO TO 12
      PP(J)=A*RO/GC*(VR-VS)/2.+(PR+PS)/2.
      VP(J)=(VR+VS)/2.+16.1*(PR-PS)/(A*RO)-FC*2.*V(J)*ABS(V(J))*DELT/D
C     CALCULATION AT POINT 2
      IF(J.NE.2) GO TO 80
   12 PP(2)=(PR+PS)/2.+A*RO/GC*(VR-VS)/2.+XCR*RO*G/(2.*GC)
      VP(2)=(VS+VR)/2.+GC/(A*RO)*(PR-PS)/2.+G*XCR/(2.*A)-2.*FC*V(2)
     1*ABS(V(2))*DELT/D
   80 CONTINUE
C     BOUNDARY CONDITIONS AT THE RESERVOIR
      VS= V(1)+DELT/DELTX*A*(V(2)-V(1))
      PS=PT(1)+DELT/DELTX*A*(PT(2)-PT(1))
      VP(1)=VS+GC/(A*RO)*(PT(1)-PS)+G*DELT-2.*FC*VS*ABS(VS)*DELT/D
C     BOUNDARY  CONDITIONS  AT  THE  VALVE
      IF(T.GT..0968)GO TO 16
      IF(T.GT.0..AND.T.LE..0242) CV=20.5-405.*T
      IF(T.GT..0242.AND.T.LE..0323) CV=17.3-272.5*T
      IF(T.GT..0323.AND.T.LE..0404)CV=14.6-190.5*T
      IF(T.GT..0404.AND.T.LE..0484)CV=12.4-137.5*T
      IF(T.GT..0484.AND.T.LE..0565)CV=10.35-95.5*T
      IF(T.GT..0565.AND.T.LE..0645)CV=8.15-56.6*T
      IF(T.GT..0645.AND.T.LE..0968)CV=5.5-15.5*T
   16 IF(T.GT..0968)CV=4.0
      TAU=CV/CV0
      PR=PT(11)+DELT/DELTX*A*(PT(10)-PT(11))
      VR=V(11)+DELT/DELTX*A*(V(10)-V(11))
      C1=GC*DELP0/(A*RO*(VSS**2)*(TAU**2))
      C2=VR+GC*PR/(A*RO)+G*XPC/A-2.*FC*VR*ABS(VR)*DELT/D
      VP(11)=(-1.+SQRT(1.+4.*C1*C2))/(2.*C1)
      PP(11)=(VP(11)/(VSS*TAU))**2*DELP0
C     CONDITIONS  AT  THE  TRANSDUCER
      VP(12)=VP(11)-TRANDS/DELTX*(VP(11)-VP(10))
      PP(12)=PP(11)-TRANDS/DELTX*(PP(11)-PP(10))-2.42*RO*
     1(1-TRANDS/DELTX)
      DO 15 J=1,KK
   15 V(J)=VP(J)
      DO 40 J=2,KK
      PT(J)=PP(J)
   40 PP(J)=PP(J)/144.
      PP(1)=PP(12)=PINOT
C     PRINTOUT  CONTROL
      IF(U.GT.500)  GO TO 10
      IF(U/5*5.EQ.U) GO TO 20
      GO TO 30
   10 STOP
      END
$ENTRY
```

VALVE CHARACTERISTICS (7-10 CLOSING)

```
55          PR=PT(J)+DELT/DELTX*A*(PT(J-1)-PT(J))
56          PS=PT(J)+DELT/DELTX*A*(PT(J+1)-PT(J))
57          IF(J.EQ.2) GO TO 12
58          PP(J)=A*RO/GC*(VR-VS)/2.+(PR+PS)/2.
59          VP(J)=(VR+VS)/2.+16.1*(PR-PS)/(A*RO)-FC*2.*V(J)*ABS(V(J))*DELT/D
      C  CALCULATION AT POINT 2
60          IF(J.NE.2) GO TO 80
61       12 PP(2)=(PR+PS)/2.+A*RO/GC*(VR-VS)/2.+XCR*RO*G/(2.*GC)
62          VP(2)=(VS+VR)/2.+GC/(A*RO)*(PR-PS)/2.+G*XCR/(2.*A)-2.*FC*V(2)
           1*ABS(V(2))*DELT/D
63       80 CONTINUE
      C  BOUNDARY CONDITIONS AT THE RESERVOIR
64          VS= V(1)+DELT/DELTX*A*(V(2)-V(1))
65          PS=PT(1)+DELT/DELTX*A*(PT(2)-PT(1))
66          VP(1)=VS+GC/(A*RO)*(PT(1)-PS)+G*DELT-2.*FC*VS*ABS(VS)*DELT/D
      C  BOUNDARY  CONDITIONS  AT  THE  VALVE
67          IF(T.GT..0968) GO TO 16
68          IF(T.GT.0..AND.T.LE..0484)CV=94.-589.*T
69          IF(T.GT..0484.AND.T.LE..0645)CV=190.-2575.*T
70          IF(T.GT..0645.AND.T.LE..0726)CV=57.-509.*T
71          IF(T.GT..0726.AND.T.LE..0807)CV=35.5-217.*T
72          IF(T.GT..0807.AND.T.LE..0968)CV=31.75-173.*T
73       16 IF(T.GT..0968) CV=15.
74          TAU=CV/CVO
75          PR=PT(11)+DELT/DELTX*A*(PT(10)-PT(11))
76          VR=V(11)+DELT/DELTX*A*(V(10)-V(11))
77          C1=GC*DELPO/(A*RO*(VSS**2)*(TAU**2))
78          C2=VR+GC*PR/(A*RO)+G*XPC/A-2.*FC*VR*ABS(VR)*DELT/D
79          VP(11)=(-1.+SQRT(1.+4.*C1*C2))/(2.*C1)
80          PP(11)=(VP(11)/(VSS*TAU))**2*DELPO
      C  CONDITIONS  AT  THE  TRANSDUCER
81          VP(12)=VP(11)-TRANDS/DELTX*(VP(11)-VP(10))
82          PP(12)=PP(11)-TRANDS/DELTX*(PP(11)-PP(10))-2.42*RO*,
           1(1-TRANDS/DELTX)
83          DO 15 J=1,KK
84       15 V(J)=VP(J)
85          DO 40 J=2,KK
86          PT(J)=PP(J)
87       40 PP(J)=PP(J)/144.
88          PP(13)=PP(12)-PTNOT
      C  PRINTOUT  CONTROL
89          IF(U.GT.500)  GO TO 10
90          IF(U/5*5.EQ.U) GO TO 20
91          GO TO 30
92       10 STOP
93          END

      $ENTRY
```

VALVE CHARACTERISTICS (3-7.7 CLOSING)